

INFORMATION TO USERS

This manuscript has been reproduced from the microfilm master. UMI films the text directly from the original or copy submitted. Thus, some thesis and dissertation copies are in typewriter face, while others may be from any type of computer printer.

The quality of this reproduction is dependent upon the quality of the copy submitted. Broken or indistinct print, colored or poor quality illustrations and photographs, print bleedthrough, substandard margins, and improper alignment can adversely affect reproduction.

In the unlikely event that the author did not send UMI a complete manuscript and there are missing pages, these will be noted. Also, if unauthorized copyright material had to be removed, a note will indicate the deletion.

Oversize materials (e.g., maps, drawings, charts) are reproduced by sectioning the original, beginning at the upper left-hand corner and continuing from left to right in equal sections with small overlaps.

**ProQuest Information and Learning
300 North Zeeb Road, Ann Arbor, MI 48106-1346 USA
800-521-0600**

UMI[®]



**NOISE AND DISORDER EFFECTS ON FRONT
PROPAGATION IN NON-LINEAR MEDIA**

BY

SAEED MAJED TURKI AL-MARZOUG

A Thesis Presented to the
DEANSHIP OF GRADUATE STUDIES

KING FAHD UNIVERSITY OF PETROLEUM & MINERALS

DHAHRAN, SAUDI ARABIA

In Partial Fulfillment of the
Requirements for the Degree of

MASTER OF SCIENCE

In

PHYSICS

DECEMBER 2002

UMI Number: 1412286

UMI[®]

UMI Microform 1412286

Copyright 2003 by ProQuest Information and Learning Company.

All rights reserved. This microform edition is protected against
unauthorized copying under Title 17, United States Code.

ProQuest Information and Learning Company

300 North Zeeb Road

P.O. Box 1346


Ann Arbor, MI 48106-1346

**KING FAHD UNIVERSITY OF PETROLEUM AND MINERALS
DHAHRAN 31261, SAUDI ARABIA**

DEANSHIP OF GRADUATE STUDIES

This thesis, written by Saeed Majed AL-Marzoug under the direction of his Thesis Advisor and approved by his Thesis Committee, has been presented and accepted by the Dean of the graduate studies, in partial fulfillment of the requirement for the degree of **MASTER OF SCIENCE IN PHYSICS**.

Thesis Committee



Professor H. Bahlouli
Chairman



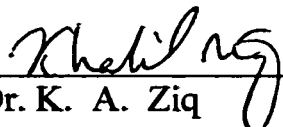
Dr. A. AL-Sunaidi
Member



Dr. S. AL-Amoudi
Member




Professor H. Mavromatis
Member



Dr. K. A. Ziq
Member



Department Chairman



Dean, Deanship of Graduate studies

Dr. Osama Jannadi

25-1-2003
Date



*This thesis is dedicated to my wife Umm
Mohammed for her encouragement and support and
my delighted son Mohammed.*

Acknowledgement

Acknowledgement is due to King Fahd University of Petroleum and Minerals for support of this research.

Thanks and appreciations are warmly due to Professor Hocine Bahlouli who introduced me to this subject and served as my major advisor. I also wish to thank the members of my Thesis committee Drs Saeed AL-Amoudi, Abdullah AL-Sunaidi, Harry Mavromatis, Khaleel A. Ziq for their useful comments and discussions. Finally, I would like to thank the Physics Department of the King Fahd University of Petroleum and Minerals for the facilities, they provided to complete this thesis.

TABLE OF CONTENTS

List of Figures	vi
Thesis Abstract (English)	viii
Thesis Abstract (Arabic)	ix
CHAPTER 1: INTRODUCTION	1
CHAPTER 2: FLUCTUATIONS AND DYNAMICS	4
2.1. Brownian Motion.....	5
2.1.1 Short time limit.....	7
2.1.2 Long time limit.....	9
2.2. Langevin Equation.....	10
2.3. Numerical Methods.....	13
2.3.1 Random noise.....	17
2.3.2 Illustrative simulations.....	18
CHAPTER 3: FRONT PROPAGATION	23
3.1 Introduction.....	23
3.2 Properties of the front solution.....	25
3.3 Stability of the front solution.....	32
3.4 Numerical computation of reaction diffusion equation.....	34
CHAPTER 4: NOISE EFFECT ON FRONT PROPAGATION	41
4.1 Internal Noise.....	42
4.2 External Noise.....	47
CHAPTER 5: DISORDER EFFECT ON FRONT PROPAGATION	57
Model and Numerical Results.....	59
CHAPTER 6: CONCLUSION	66
APPENDIX A: STABILITY OF REACTION DIFFUSION EQUATION	69
References	71
Vita	75

LIST OF FIGURES

Figure 1:	Histogram of the distribution of Gaussian numbers created after generating N random numbers. The exact Gaussian distribution (dot line) is also plotted	20
Figure 2:	Histogram of the distribution of Gaussian numbers created after generating N random numbers. The exact Gaussian distribution (dot line) is also plotted	20
Figure 3:	Histogram of the distribution of Gaussian numbers created after generating N random Numbers. The exact Gaussian distribution (dot line) is also plotted	21
Figure 4:	The mean square displacement of a Langevin equation as function of time	21
Figure 5:	The mean square displacement of Langevin equation as function of time where $t \ll \frac{1}{\gamma}$ in short time limit	22
Figure 6:	The mean square velocity of a Langevin equation as a function of time	22
Figure 7:	Potential $U(\phi) = \frac{1}{2}\phi^2 - \frac{1}{3}\phi^3$. Equation (3.4) for a profile moving with steady state velocity v can be interpreted as the equation for a particle subject to friction moving down the potential	38
Figure 8:	Velocity against ξ . The Solid line is numerical simulation and the dot line is theoretical value	38
Figure 9:	Shape of the front at different time	39
Figure 10:	$Ln(\zeta)$ as function of time to reach the unity	39
Figure 11:	Velocity of the front as function of time. The solid line is to indicate the $v=2.0$ and the symbols are numerical simulation	40
Figure 12:	Velocity of the front as function of $1/t$	40
Figure 13:	Front propagation with internal noise and with intensity $\epsilon=0.001$, we show the function $\langle \phi(x_0(t), t) \rangle$ at five equally spaced times between $t=10$ to $t=100$. Symbols are indicate eyes	45
Figure 14:	The quantity x_0 obtained from the data in Fig.13 as function of $t^{\frac{1}{2}}$	45

Figure 15:	Numerical results for $\langle \phi(x, t) \rangle$ at different noise intensity ε and fixed value of time $t=50$	46
Figure 16:	Results for x_0 at very low noise levels, extracted from data such as that shown in in Fig.13	46
Figure 17:	Characteristic time t_0 as function of noise intensity $-\ln \varepsilon$, extracted from Fig.16	48
Figure 18:	Front propagation shape as function of space with different external noise intensity ε and a fixed value of time $t=100$	52
Figure 19:	Front velocity vs time for several values of noise intensity ε	52
Figure 20:	Front velocities vs noise intensity ε . The symbols represent the numerical results. The straight line is a least squares liner fit of v vs ε	53
Figure 21:	Width of the front as function of time when the noise strength is 0.5	53
Figure 22:	Width of the front as function of noise intensity	54
Figure 23:	Front velocities vs $1/t$ with several values of noise intensity ε	56
Figure 24:	Front propagation when a single impurity when the strength is 0.5 at $x=565$	61
Figure 25:	Front propagation as function of space with different disorder intensity β . The concentration of impurities is fixed to 5% at $t=100$	61
Figure 26:	Front amplitude as function of space with different disorder intensity β . The concentration of impurities is fixed to 5% at $t=100$	62
Figure 27:	Velocity of the front propagation as function of disorder intensity β . The concentration of impurities is fixed to 5% at $t=100$	62
Figure 28:	Amplitude of the front propagation as function of disorder intensity β . The concentration of impurities is fixed to 5% at $t=100$	63
Figure 29:	Width of the front propagation as function of disorder intensity β . The concentration of impurities is fixed to 5% at $t=100$	63
Figure 30:	Velocity of the front propagation as function of impurity concentration. The intensity of impurity potential is 0.1	64
Figure 31:	Amplitude of the front propagation as function of impurity concentration. The intensity of impurity potential is 0.1	64
Figure 32:	Width of the front propagation as function of impurity concentration. The intensity of impurity potential is 0.1	65

ABSTRACT

NAME: SAEED MAJED AL-MARZOUG
TITLE: DISORDER AND NOISE EFFECT ON FRONT
PROPAGATION IN NONLINEAR MEDIA
FIELD: PHYSICS
DATE: DECEMBER 2002

We study the dynamics of reaction-diffusion fronts under the influence of noise and static disorder. In the absence of noise mathematically rigorous results establish that fronts propagate with constant velocity. Noise affects the front propagation in two possible ways. First, intrinsic noise modeled typically by an additive thermal noise in a Langevin type equation causes a sharp crossover from ballistic to diffusive motion of the front. Second, external noise is introduced through the fluctuations of a control parameter leading to a multiplicative noise in the stochastic partial differential equation. The external noise increases the mean propagation velocity of the front. Finally, we consider the influence of static disorder of the properties of front propagation. Static disorder is found, to our surprise, to enhance the speed of propagation linearly with impurity potential and concentration strength.

**MASTER OF SCIENCE DEGREE
KING FAHD UNIVERSITY OF PETROLEUM AND MINERALS
DHAHRAN, SAUDI ARABIA
DECEMBER 2002**

خلاصة الرسالة

الاسم: سعيد ماجد تركي آل مرزوق

عنوان الرسالة: أثر عدم الانتظام والضجيج على مقدمة انتشار الاضطراب في الأوساط غير الخطية.

التخصص: فيزياء

التاريخ: شوال - ١٤٢٣هـ

قمنا بدراسة ديناميكية تفاعلات انتشار مقدمات الاضطراب تحت تأثير الضجيج وعدم الانتظام الساكن. عند عدم وجود الضجيج فإن النتائج الرياضية الدقيقة توضح أن مقدمة التخلخل تنتشر بسرعة ثابتة. الضجيج يؤثر في مقدمة الاضطراب بطريقتين. الأولى بطريقة نموذج الضجيج الداخلي، وبالتحديد بإضافة الضجيج الحراري في المعادلة المشابهة لمعادلة لانجفين والتي ينتج عنها تحول حاد لحركة مقدمة التخلخل من الحركة المشابهة لحركة القذيفة إلى الحركة المنتشرة. والثانية فإن الضجيج الخارجي يؤدي إلى زيادة السرعة المتوسطة لمقدمة التخلخل. أخيراً، قمنا بدراسة أثر عدم الانتظام الساكن لخواص مقدمة التخلخل. نتيجة لذلك فقد وجد وبشكل مذهل أن عدم الانتظام الساكن يؤدي إلى دعم بقاء العلاقة بين سرعة انتشار التخلخل علاقة خطية مع الجهد الناتج عن الشوائب ومدى التكنف.

درجة الماجستير في العلوم

جامعة الملك فهد للبترول والمعادن

الظهران، المملكة العربية السعودية

شوال، ١٤٢٣هـ (ديسمبر ٢٠٠٢)

CHAPTER 1

Introduction

Interfaces between two distinct material phases are perhaps the most obvious feature in nature. The formation of crystals in solids such as snowflakes or metal alloys can be described by the evolving surface which separates the solid phase from the surrounding liquid melt.

Sharp interface models PDE assume that the interface is geometrically a surface and that continuum variables such as temperature pressure satisfy certain conditions on these surfaces. Such models are, however, inadequate for two reasons. The first of these is that the interface really isn't sharp in most cases. It simply represents a very narrow but finite layer between two phases. This possibility is most evident in binary fluids which are slightly miscible since there is mixing near the interface [1]. The second and more problematic feature of these models is that they are difficult to simulate numerically. Tracking interfaces in a computational setting is complicated because they frequently undergo topological transitions by splitting or merging.

A solution to both of these problems is to introduce a new continuum variable usually called order parameter which, takes distinct values in each phase, but varies smoothly across

the interface. The interface is then only described implicitly by the transition layer of the order parameter. The dynamical equations of diffuse models usually take a familiar form, that of parabolic systems of partial differential equations.

Diffuse models have two obvious advantages. Analytically, one would hope that such models would yield insight into the true nature of topological transitions. The second advantage is a more practical one, which is the ability to compute interface motion without explicitly tracking the interface. Even when the order parameter has no physical relevance we may obtain useful results if our only goal is numerical approximation [2].

We should also point out some of the disadvantages of diffuse interfaces. Their most problematic feature is that the width of the transition layer must necessarily be small. In computations this leads to considerable difficulty in obtaining enough resolution of large gradients. The other potential problem comes from the fact that diffuse models are only an approximation when the sharp interface dynamics is desired [3].

The study of the influence of noise in several systems continues being an active field of research both experimentally [4] and theoretically [5]. The amplification of fluctuations seems to be an important ingredient in the explanation of phenomena such as secondary fingering in Hele-Shaw fingers [6], and directional solidification and dendritic growth [7]. The studies on several systems have shown that in most cases the intensity of thermal noise is not large enough to account for the observed dynamics [5], so other sources of noise have to be invoked. In any case external fluctuations can be imposed on a system through a control parameter and in a certain degree, are unavoidable when a system is kept out of equilibrium. In this context, there are some experiments in which isolated or periodic

heat pulses [8] or modulation of some other parameter [4] have been employed. Also, the introduction of fluctuations in experimentally controlled way seems to be an important step in order to clarify the role of noise.

The aim of this thesis is to examine the effects of noise and disorder on front propagation. The nature of this work is to find out how noise and disorder change the speed, width and shape of the front propagation. Our main contribution is introducing static disorder into the front and compare the results with noise effect. Static disorder is found, to our surprise, to enhance the speed of propagation linearly with impurity potential and concentration strength.

The content of this thesis is organized as follows. In chapter 2, we study the Brownian motion of a particle and address the Langevin equation which is a simple model of that motion. In chapter 3, we extend the analysis of chapter 2 to front propagation in one dimension and rigorously establish some existence criteria. In chapter 4, we study the noise effect on front propagation by solving numerically the appropriate diffusion reaction equation. We will find the effects the noise into the front including both internal noise and external noise. In chapter 5, we study the statics disorder effect on front propagation. Finally, we comment on results front propagation and present our conclusion.

CHAPTER 2

Fluctuations and Dynamics

Fluctuation processes are basic to the whole field of non-equilibrium phenomena. The thermodynamic variables describing a system have small random deviations from their mean values, which are neglected in ordinary thermostatics. An estimate of the deviations from the most probable values of the thermodynamic quantities enables one to specify the conditions for the validity of thermodynamic observations and calculations [9].

Besides this theoretical interest, there are two other reasons for studying fluctuation phenomena. First, with the availability of refined and sensitive experimental techniques, it was possible to study fluctuation phenomena in many areas. Light scattering experiments or measurements of the line width in magnetic resonance experiments are basically studies of fluctuations [10]. The study of fluctuations in reaction rates may yield much more useful information not available from the study of equilibrium reaction constants [11]. Second, the concept of fluctuations is essential for the study of transport phenomena [10].

2.1 Brownian Motion

In 1828, Robert Brown observed that tiny grains of pollen immersed in water underwent a perpetual random motion. He went on to observe this effect in a whole range of powdered substances [11]. Brown's conclusion was that the motion was due to some "life force" in all inorganic matter. Today the importance of his work is in the universality of the effect. It was Einstein in 1905, who explained the origin of the motion as arising from the constant bombardment of the particles (the atoms or molecules) of the fluid in which it is immersed [12]. The key point about Brownian motion is that it is the motion of a macroscopic body arising from impacts from atoms/molecules of the surrounding fluid. The macroscopic body, which nevertheless might be quite small, might be pollen grains in water, smoke particles in air, particles of ink pigment in water or the mirror of a traditional galvanometer. The random motion of all these systems may be observed [13].

For simplicity we shall consider the motion of a Brownian particle in one dimension. The generalization to two and three dimensions is straightforward. We shall investigate the mean square displacement of the particle. At this stage we consider the *kinematics* of the particle. That is, we will treat things at a descriptive (but quantitative) level.

The distance travelled by the Brownian particle in a given time may be found by integrating over its velocity:

$$x(t) = \int_0^t v(\tau) d\tau. \quad (2.1)$$

Here $v(\tau)$ is the particle's velocity at time τ . The square of the displacement is then

$$x^2(t) = \int_0^t d\tau_1 \int_0^t d\tau_2 v(\tau_1)v(\tau_2)$$

so the mean square displacement is

$$\langle x^2(t) \rangle = \int_0^t d\tau_1 \int_0^t d\tau_2 \langle v(\tau_1)v(\tau_2) \rangle. \quad (2.2)$$

We see that the mean square displacement is given in terms of the velocity autocorrelation function

$$G_v(\tau_1 - \tau_2) = \langle v(\tau_1)v(\tau_2) \rangle. \quad (2.3)$$

Here we have used the subscript v to indicate that it is the autocorrelation function of the velocity. The stationary nature of the random velocity (a consequence of thermal equilibrium) is indicated by the argument $(\tau_1 - \tau_2)$. This allows us to take a further step in the expression for the mean square displacement. We may change variables in the double integral to

$$\tau = \tau_1 - \tau_2 \quad (2.4)$$

$$T = \tau_1 + \tau_2$$

The autocorrelation function will change negligibly from its initial value for times much longer τ_v . So when we consider times much shorter than τ_v , we may replace $G_v(t)$ by $G_v(0)$ in the integral expression for $\langle x^2(t) \rangle$. In this case $G_v(0)$ comes out of the integral and we have

$$\langle x^2(t) \rangle = 2G_v(0) \int_0^t (t - \tau) d\tau. \quad (2.8)$$

Now the integral may be evaluated simply, giving

$$\langle x^2(t) \rangle = G_v(0)t^2. \quad (2.9)$$

The mean square displacement is proportional to the square of the time interval. We may write our result as

$$\langle x^2(t) \rangle = \langle v^2 \rangle t^2. \quad (2.10)$$

This indicates that the Brownian particle is moving essentially freely; at these short times there have not been sufficient atomic impacts to have any significant effect on the particle's motion. This is referred to as the *ballistic* regime [15].

2.1.2 Long time limit

Limiting case is the long time limit where $t \gg \tau_v$. In this case

$$G_v(t) \approx 0 \quad t \gg \tau_v; \quad (2.11)$$

the autocorrelation function will have decayed to zero at long times. So when we consider times much longer than τ_v , $G_v(t)$ will be very small and in the expression for $\langle x^2(t) \rangle$ we will make a negligible error by extending the upper limit of the integral to infinity.

$$\langle x^2(t) \rangle = 2 \int_0^\infty (t - \tau) G_v(\tau) d\tau. \quad (2.12)$$

The integral may be rearranged as

$$\langle x^2(t) \rangle = 2t \int_0^\infty G_v(\tau) d\tau - 2 \int_0^\infty \tau G_v(\tau) d\tau. \quad (2.13)$$

The second term (independent of time) is negligible compared with the first at long times, so we conclude that in the long time limit

$$\langle x^2(t) \rangle = 2t \int_0^\infty G_v(\tau) d\tau. \quad (2.14)$$

Now we see that the mean square displacement of the Brownian particle is proportional to time (rather than the t^2 of the ballistic regime). We recall that a mean square displacement proportional to time is a characteristic of a diffusive process. And in fact in $1D$, the solution of the diffusion equation gives directly

$$\langle x^2(t) \rangle = 2Dt \quad (2.15)$$

where D is the diffusion coefficient [13].

Thus we conclude that in the long time limit the motion of the Brownian particle is diffusive and its diffusion coefficient is given by

$$D = \int_0^{\infty} G_v(\tau) d\tau . \quad (2.16)$$

The diffusion coefficient is given by the area under the velocity autocorrelation function. The long time limit, when $t \gg \tau_v$, is called the *diffusive* regime [16].

2.2 Langevin Equation

The task of examining the dynamics of Brownian motion was initiated by Langevin in 1908 [12]. Langevin wrote down a macroscopic equation of motion for the Brownian particle. Essentially this was an equation of the form $F = ma$, but Langevin's important

It is convenient to make a simplification by the substitutions:

$$\begin{aligned} A(t) &= \frac{f(t)}{M} \\ \gamma &= \frac{1}{M\alpha} \end{aligned} \tag{2.19}$$

then the Langevin equation becomes

$$\frac{dv(t)}{dt} + \gamma v(t) = A(t). \tag{2.20}$$

By similar arguments we can now examine the mean square velocity. A key result then follows when we exploit the equipartition theorem to relate the equilibrium mean square velocity of the Brownian particle to the temperature of its surrounding medium. The expression for the mean square velocity is

$$\langle v^2(t) \rangle = \frac{\epsilon}{\gamma} (1 - e^{-2\gamma t}) \tag{2.21}$$

And in the long time limit this takes on the time-independent value

$$\langle v^2(t) \rangle = \frac{\epsilon}{\gamma} \tag{2.22}$$

based on predictor corrector [65] and schemes based on Runge-Kutta method [25–27].

In the literature it is possible to find algorithms which share the same basic idea with the one I will mention here. Another approach has been proposed by Fox [28], where the deterministic force appearing in the SDE is integrated by a Runge-Kutta whereas the stochastic force is integrated using a Taylor expansion. The algorithms proposed in reference [25] extend the Fox approach to an implicit Runge-Kutta method treatment of the stochastic force is integrated using a Taylor expansion. The algorithms proposed in reference [26] extend the Fox approach to an implicit Runge-Kutta treatment of the stochastic force.

In this section we want to study how to handle numerically the Langevin equation. Let us consider a one variable stochastic differential equation:

$$\frac{dv(t)}{dt} = F(v(t)) + \eta(t) \quad (2.25)$$

where $F(v(t))$ is a sufficiently smooth (differentiable) function and $\eta(t)$ is a Gaussian distributed random variable of mean zero and correlation:

$$\langle \eta(t)\eta(\hat{t}) \rangle = D\delta(t - \hat{t}) \quad (2.26)$$

We will use the Euler method to solve equation (2.25). The algorithm generates a recursion relation that will allow us to compute $v(t+h)$ given $v(t)$, where h is the integration step. This is the same structure as in ordinary differential equations in which numerical methods

do not give the solution for every value of time t but only at regular intervals $t_n = t_0 + nh, n = 0, 1, \dots$ separated by an integration step h . In order to find the recursion relation we integrate (2.25) between t_n and $t_n + h$ to obtain (we have taken $t_0 = 0$ to simplify the notation):

$$v(t_n + h) - v(t_n) = \int_{t_n}^{t_n+h} ds F(v(s)) + \int_{t_n}^{t_n+h} ds \eta(s) \quad (2.27)$$

the first term on the right hand side of this equation can be approximated by

$$\int_{t_n}^{t_n+h} ds F(v(s)) = hF(v(t_n)) + o(h^2) \quad (2.28)$$

The second term is a Gaussian variable since it is the integral of a Gaussian variable. Hence, its statistical properties are completely determined by the mean value and the correlations. Lets define the random variable:

$$w_h(t) = \int_t^{t+h} ds \eta(s) \quad (2.29)$$

whose mean value is:

$$\langle w_h(t) \rangle = \int_t^{t+h} ds \langle \eta(s) \rangle = 0 \quad (2.30)$$

and whose correlations are given by:

$$\langle w_h(t)w_h(\hat{t}) \rangle = \int_t^{t+h} ds \int_{\hat{t}}^{\hat{t}+h} du \langle \eta(s)\eta(u) \rangle = \int_t^{t+h} ds \int_{\hat{t}}^{\hat{t}+h} du D\delta(s-u) \quad (2.31)$$

The important thing to notice is that for the time t_n that appears in the recursion relation (2.27), one has $\langle w_h(t)w_h(\hat{t}) \rangle = Dh\delta(t-\hat{t})$, so that the variables $w_h(t_n)$ are independent, Gaussian, random variables of zero mean and variance $\langle w_h(t_n)^2 \rangle = Dh$. Hence they can be written as

$$w_h(t_n) = \sqrt{Dh}X^{(n)} \quad (2.32)$$

where $X^{(n)}$ are independent Gaussian variables of mean zero and variance unity which can be generated, for instance, by the Box-Muller-Wiener method [28].

The final recursion relation reads:

$$\begin{aligned} v^{(0)} &= v_0 \\ v^{(n+1)} &= v^{(n)} + hF^{(n)} + \sqrt{Dh}X^{(n)} \end{aligned} \quad (2.33)$$

It is possible but very tedious to develop higher order algorithms. It is good that very rarely does one really need them. This is so because, in general, one has to solve numerically the Langevin equation and average the results for over different realizations of the noise.

This generates a source of statistical errors coming from the averages which are, in many cases, greater than the systematic errors due to the order of convergence of the numerical method. So it is usually better to spend the computer time in reducing the statistical errors by increasing the number of samples in the average rather than using a more complicated, higher order, algorithm.

2.3.1 Random noise

Fluctuations in nonequilibrium statistical mechanics are usually modeled by adding a stochastic term to the macroscopic and deterministic differential equation governing the dynamics of the system under consideration. By doing this one obtains what is called the Langevin equation or stochastic differential equation :

$$\frac{\partial \phi(r, t)}{\partial t} = F(\phi(r, t)) + \eta(r, t) \quad (2.34)$$

The first term on the right-hand side is a deterministic force. The term $\eta(r, t)$ is a random force called noise, which is usually assumed to be Gaussian, and accounts for either internal degrees of freedom, or fluctuations in the constraints imposed externally on the system. In the first case the noise is called an internal noise, and typically represents thermal fluctuations. In the second case we have an external noise, whose properties could be controlled experimentally.

In general, internal noise has been assumed to be white to a very good approximation. This means that the value of the random field at a given point and time does not depend

on its value at other points or times:

$$\langle \eta(r, t) \eta(\hat{r}, \hat{t}) \rangle = 2\epsilon \delta(r - \hat{r}) \delta(t - \hat{t}) \quad (2.35)$$

where ϵ is the intensity of the noise and $\langle \rangle$ denotes an average over the probability distribution of the random field. The generation of a Gaussian random number is usually done by the Box-Muller-Wiener (BMW) algorithm: if ξ_1 and ξ_2 are two random numbers uniformly distributed in the interval $[0, 1]$, then the numbers x_1 and x_2 given by

$$\begin{aligned} x_1 &= \sqrt{-2 \log(\xi_1)} \sin(2\pi\xi_2) \\ x_2 &= \sqrt{-2 \log(\xi_1)} \cos(2\pi\xi_2) \end{aligned} \quad (2.36)$$

are random numbers distributed according to a Gaussian distribution of mean 0 and variance

1. Random numbers z of mean μ and variance σ^2 are obtained by the linear transformation

$$z = \mu + \sigma x \quad [29].$$

2.3.2 Illustrative simulations

Generators of random numbers are used to make long sequences. The sequence is then tested by its ability to reproduce the given auto-correlation function. In the following figures, in order to test the algorithm, we have generated several of realizations by using the Gasdev algorithm [30].

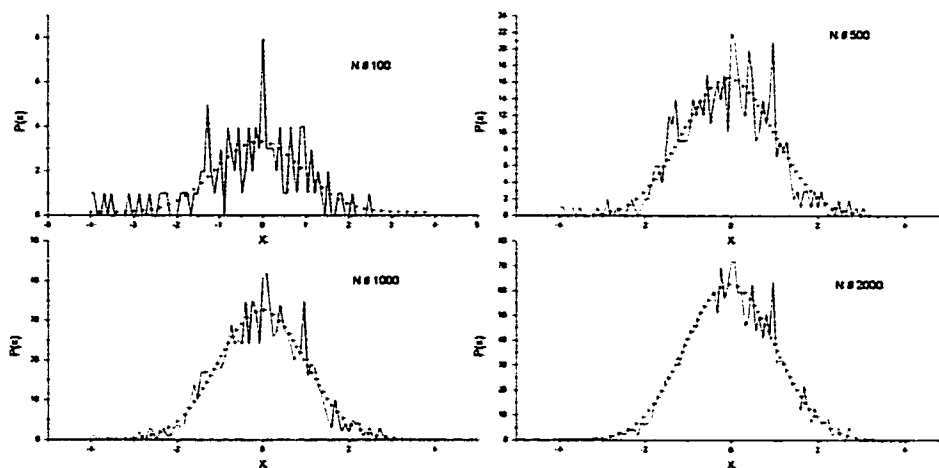


Figure 1: Histograms of the distribution of Gaussian numbers created after generating N random numbers. The exact Gaussian distribution (dot line) is also plotted.

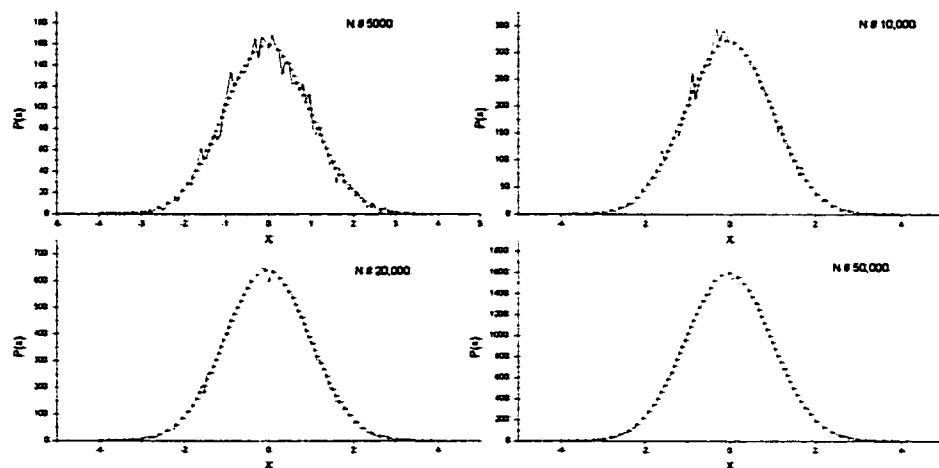


Figure 2: Histograms of the distribution of Gaussian numbers created after generating N random numbers. The exact Gaussian distribution (dot line) is also plotted.

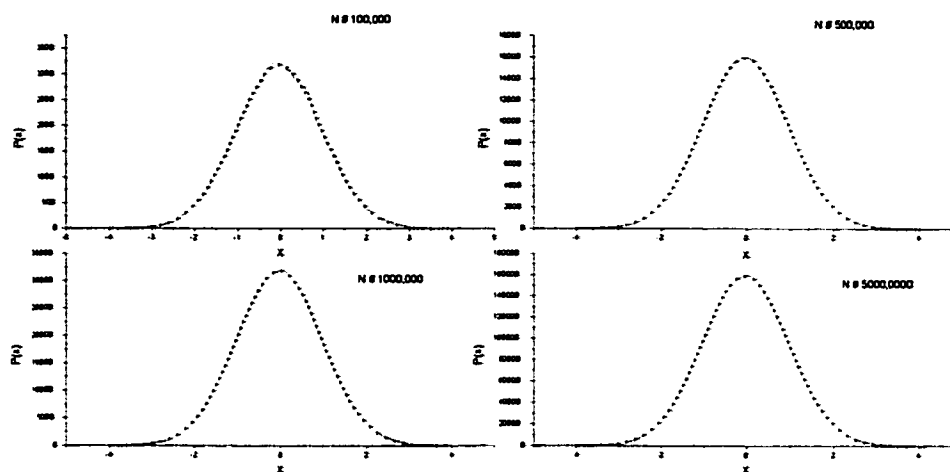


Figure 3: Histograms of the distribution of Gaussian numbers created after generating N random numbers. The exact Gaussian distribution (dot line) is also plotted.

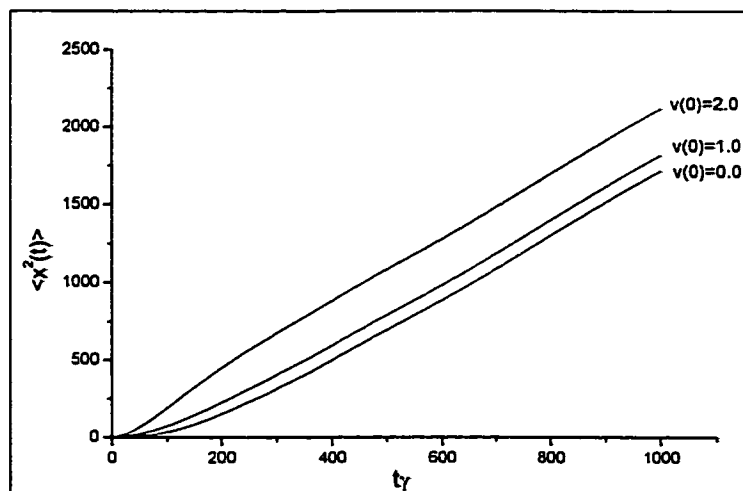


Figure 4: The mean square displacement of a Langevin equation as function of time.

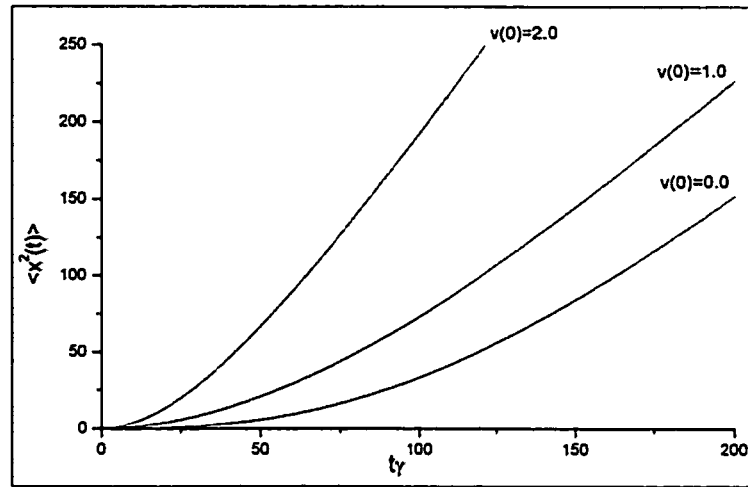


Figure 5: The mean square displacement of Langevin equation as function of time where $t \ll \frac{1}{\gamma}$ in short time limit

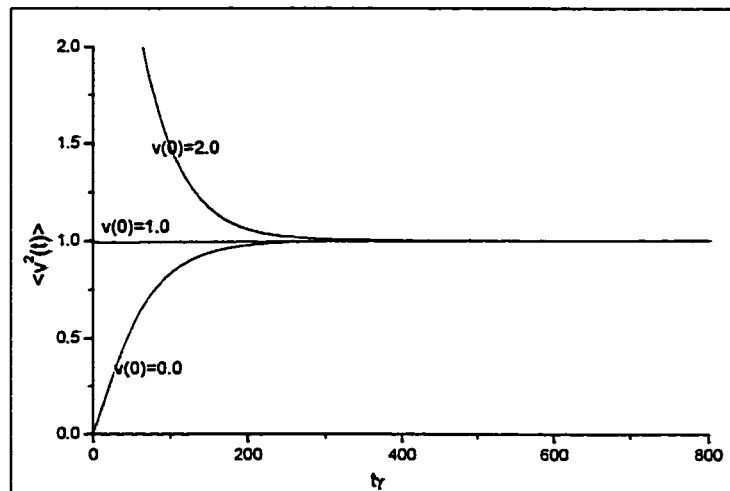


Figure 6: The mean square velocity of a Langevin equation as a function of time

CHAPTER 3

Front propagation

3.1 Introduction

Nonlinear phenomena in physics constitute the rule rather than the exception. Linear phenomena are limited to weak driving forces and consequently small responses of a system which remains close to its equilibrium state. The study of nonlinear phenomena has recently advanced due to the huge advances in nonlinear computations. In the 1960's when physics produced, say, a nonlinear differential equation that we could not solve analytically, we usually had to drop the problem. Nowadays, computers are becoming an essential tool for research and with their help nonlinear phenomena are studied in great details. A large number of problems of current interest in the area of nonequilibrium statistical mechanics may be formulated in terms of nonlinear partial differential equations which may contain, in addition to a deterministic part, some noise source terms [31].

Reaction-diffusion systems refer to the class of time-dependent partial differential equations which contains a local (in space) 'reaction' part and a nonlocal 'diffusion' part. These

equations are an abstract model for pattern formation but in many cases have direct applications in the fields of developmental biology, chemistry, optics, and other branches of applied mathematics. For biological and chemical systems, for example, reaction-diffusion equations represent a reduced description of a complicated set of reactions. The important aspect of all of the applications is that the simple combination of reactions plus transport due to diffusion is sufficient to produce a large variety of interesting patterns [16].

Fronts in reaction-diffusion partial differential equations have received the interest of both mathematicians and physical scientists. A front is a propagating interface between two different steady states and can be viewed physically as a balance between diffusive forces coupling different points in the field, and reactive forces which move the system from stable to unstable states. Front propagation motion occurs in many scientific areas such as chemical kinetics [32], combustion [33], biology and [34]. In spite of these different applications, the basic phenomena can all be modeled using nonlinear parabolic partial differential equations (PDEs) or systems of such equations. Since the pioneering work of Fisher [35] in 1937 on traveling fronts in reaction-diffusion equations, the field has gone through enormous growth and development. However, studies of fronts in nonlinear media have been more recent. Nonlinear medias are always present in natural environments, such as fluid convection effects in combustion, noise effects in biology, and deposition processes. One of the fundamental questions that scientists need to understand is how nonlinear media influence the characteristics of front propagation such as front speeds, front profiles, and front locations. Our goal here is to give a review of recent results on front propagation in nonlinear media in a coherent and motivating manner. We begin in section 2 with the well

studied reaction diffusion equations and explain the basic properties of their solutions. We will investigate the perturbations of initial condition to do with profile of the front.

3.2 Properties of the front solution

Here we consider a front propagating between a stable and unstable state. The theory of this phenomenon reveals some subtleties and surprises, the main one being that a continuum set of front velocities and shapes exists. The question is therefore to find out what selects the physical solutions [36, 37]. We will consider a simple example and try to explain the main physical ideas.

The invasion of an unstable state by a stable state seems to have been first considered by Fisher in the thirties as a problem in population dynamics. His equation also describes the logistic growth diffusion process and has the form

$$\frac{\partial \phi(x, t)}{\partial t} = D \frac{\partial^2 \phi(x, t)}{\partial x^2} + k\phi \left(1 - \frac{\phi}{\kappa}\right) \quad (3.1)$$

where $D(> 0)$ is a diffusion constant, $k(> 0)$ is the linear growth rate, and $\kappa(> 0)$ is the carrying capacity of the environment. The term $f(\phi) = k\phi \left(1 - \frac{\phi}{\kappa}\right)$ represents a nonlinear growth rate which is proportional to ϕ [34].

The Fisher equation (3.1) is a particular case of a general model equation, called the nonlinear diffusion equation, which can be obtained, by introducing the net growth rate $f(x, t, \phi)$. The term f is also referred to a source or reaction term and it represents the

birth-death process in an ecological context [34]. This equation arises in many physical, biological [34], and chemically problems [32] involving diffusion and nonlinear growth. For example, if a chemically reacting substance is diffusion through a medium, then, its concentration $\phi(x, t)$ satisfies (3.1) where f represents the rate of increase of the substance due to the chemical reaction.

We study the Fisher equation a nonlinear model for a physical system involving linear diffusion and nonlinear growth.. It is convenient to introduce nondimensional quantities x^*, t^*, ϕ^* defined by

$$x^* = \left(\frac{k}{D}\right)^{\frac{1}{2}} x, t^* = kt, \phi^* = \kappa^{-1}\phi, \quad (3.2)$$

where $\sqrt{\frac{k}{D}}$, k^{-1} and κ represent the length scale, time scale and population scale respectively. Using (3.2) and dropping the asterisks, equation (3.1) takes the non-dimensional form,

$$\frac{\partial\phi(x, t)}{\partial t} = \frac{\partial^2\phi(x, t)}{\partial x^2} + \phi(1 - \phi) \quad (3.3)$$

For concreteness, we choose $f(\phi) = \phi - \phi^2$ as an example. Here the state $\phi = 0$ is unstable and the state $\phi = 1$ is stable. We thus consider a situation such that $\phi(x) \rightarrow 1$ for $x \rightarrow -\infty$ and $\phi(x) \rightarrow 0$ at $x \rightarrow +\infty$ [38–40]. Clearly there is a transition region between these two states. We assume that after some transients, it relaxes to a steadily

propagating front solution that we try to determine. So we look for a solution of (3.3) of the form $\phi(x, t) = \overline{\phi(x - vt)}$ such that $\phi(x) \rightarrow 1$ for $x \rightarrow -\infty$ and $\phi(x) \rightarrow 0$ at $x \rightarrow +\infty$.

Substituting in (3.3) , we obtain:

$$\frac{d^2\phi}{dx^2} = -v\frac{d\phi}{dx} - \frac{\partial U}{\partial\phi}, \quad \text{with} \quad U(\phi) = \frac{1}{2}\phi^2 - \frac{1}{3}\phi^3. \quad (3.4)$$

This is conveniently interpreted as the equation of motion of a particle in the potential $U(\phi)$, where the role of time being played by the x coordinate. See Fig. 7

The front is represented by a particle starting at $x = -\infty$ on the top of the hill at $\phi = 1$ and arriving in the bottom of the valley at $\phi = 0$ at "time" $x = +\infty$. How should the "friction" v be chosen so that such a particle motion is possible? The intuitively clear but surprising answer is that any non zero (and positive) friction is adequate; the particle will dissipate its energy and at "time" $x = +\infty$ it will rest on the bottom of the valley. So, any positive velocity corresponds a front solution. We are thus faced with a selection problem: what is the velocity of the physical propagating front? Using the mechanical analogy, it is clear that this happens for sufficiently small friction (i.e., velocity) since in this case the particle oscillates around the bottom of the well before coming to rest at $\phi = 0$ [41]. So the friction must be larger than a critical friction. In order to see it mathematically, we can determine the behavior of (3.3) near the tail $\phi = 0$ where it reduces to:

$$\frac{d^2\phi}{dx^2} = -v\frac{d\phi}{dx} - \phi. \quad (3.5)$$

Therefore, when $x \rightarrow +\infty$, the asymptotic behavior of ϕ is like $e^{-\xi x}$ with:

$$\xi^2 - v\xi + 1 = 0 \quad \text{or} \quad v = \xi + \frac{1}{\xi}. \quad (3.6)$$

For $v < 2$ this equation has two complex roots with a positive real part. So ϕ oscillates before reaching 0 as stated. On the contrary, for $v > 2$ the two roots of (3.6) are real and positive so these solutions are not obviously forbidden. The velocity is plotted against ξ in Fig. 8.

At this stage two remarks can be made:

1. In general the branch with $\xi > 1$ does not correspond to the convergence rate of a front. The reason is simply that the large x asymptotic behavior of a solution of (3.4) moving at $v > 2$ is a superposition of the two possible asymptotic modes. Therefore its convergence rate toward zero is controlled by the slowest $\xi < 1$ converging mode making the $\xi > 1$ mode unobservable.
2. The fact that v behaves like $\frac{1}{\xi}$ for small ξ is easily interpreted. This is the behavior that would be obtained for (3.3) if the diffusive term was absent. So this has nothing to do with a real propagation. It is simply the independent growth of ϕ at different points set up by the initial condition [42].

This last remark makes it clear that the velocity of the invading front depends on the initial condition and that it can be as fast as one wants if the initial condition decreases sufficiently slowly at $x \rightarrow +\infty$. The physical question is therefore to determine the front

velocity for an initial condition that decreases sufficiently rapidly as $x \rightarrow +\infty$.

If we write (3.4) as two first order equations in the "phase space" $(\phi, \psi = \frac{d\phi}{d\xi})$, we get:

$$\begin{aligned}\frac{d\phi}{d\xi} &= \psi, \\ \frac{d\psi}{d\xi} &= -v\psi + \phi(1 - \phi),\end{aligned}\tag{3.7}$$

or, equivalently,

$$\frac{d\psi}{d\phi} = \frac{-v\psi + \phi(1 - \phi)}{\psi}.\tag{3.8}$$

The singular points of this system are the solutions of the equations

$$\psi = 0, \quad -v\psi + \phi(1 - \phi) = 0\tag{3.9}$$

Thus there are two singular points $(\phi, \psi) = (0, 0) = (1, 0)$ which represent the steady states [43].

We follow the standard phase plane analysis to examine the nature of the nonlinear autonomous system given by

$$\frac{d\phi}{d\xi} = p(\phi, \psi), \quad \frac{d\psi}{d\xi} = q(\phi, \psi).$$

The matrix associated with this system at the critical point (ϕ_0, ψ_0) is

$$\frac{d}{d\xi} \begin{pmatrix} \phi \\ \psi \end{pmatrix} = A \begin{pmatrix} \phi \\ \psi \end{pmatrix}$$

where

$$A = \begin{pmatrix} p_\phi(\phi_0, \psi_0) & p_\psi(\phi_0, \psi_0) \\ q_\phi(\phi_0, \psi_0) & q_\psi(\phi_0, \psi_0) \end{pmatrix}.$$

In the present problem, the matrix A at $(0, 0)$ is

$$A(0, 0) = \begin{pmatrix} 0 & 1 \\ 1 & -v \end{pmatrix}$$

The matrix at $(1, 0)$ is

$$A(1, 0) = \begin{pmatrix} 0 & 1 \\ -1 & -v \end{pmatrix}$$

The eigenvalues λ of the matrix A at $(0, 0)$ are the roots of the equation

$$\begin{vmatrix} 0 - \lambda & 1 \\ -1 & -(v + \lambda) \end{vmatrix} = 0.$$

This equation gives the eigenvalues

$$\lambda = -\frac{1}{2} \left[v \mp \sqrt{v^2 - 4} \right] \quad (3.10)$$

diminishing oscillations about $\phi = 0$ [40].

3.3 Stability of the front solution

We examine the stability of the traveling wave solution of (3.3) in the form

$$\phi(x, t) = \Phi(\zeta), \quad \zeta = x - vt, \quad (3.12)$$

where v is the wave speed.

Such solutions are said to be asymptotically stable if a small perturbation imposed on the system at time $t = 0$ decays to zero, as $t \rightarrow \infty$. We introduce a coordinate frame moving with the wave speed v , that is, $\zeta = x - vt, t = t$, so that (3.3) reduces to the form [45]:

$$\phi_t = v\phi_\zeta + \phi_{\zeta\zeta} + \phi(1 - \phi). \quad (3.13)$$

We look for a perturbed solution of (3.13) in the form:

$$\phi(\zeta, t) = \Phi(\zeta) + \epsilon\theta(\xi, t), \quad (3.14)$$

where ϵ ($0 < \epsilon \ll 1$) is a small parameter and the second term represents a small perturbation from the given basic solution $\Phi(\zeta)$. The perturbed state $\theta(\xi, t)$ is assumed to have

compact support in the moving frame, that is , $\theta(\xi, t) = 0$ for $|\zeta| \geq a$ for some finite $a > 0$.

We substitute (3.14) into (3.13) to find the equation for the perturbed quantity, to order ϵ ,

$$\theta_t = c\theta_{\zeta\zeta} + \theta_{\zeta\zeta} + (1 - 2\Phi)\theta. \quad (3.15)$$

We next seek solutions of this equation in the form:

$$\theta(\zeta, t) = V(\zeta)e^{-\lambda t}. \quad (3.16)$$

Substituting this solution into (3.15) gives the following linear eigenvalue problem

$$\frac{d^2V}{d\zeta^2} + v\frac{dV}{d\zeta} + (\lambda + 1 - 2\Phi)V = 0, \quad (3.17)$$

where the growth factor λ is considered an eigenvalue. Since the original perturbed state has a compact support, we may take the boundary condition on $V(\zeta)$ as $V(\pm a) = 0$. According to the general theory of eigenvalue problems, the perturbation will grow in time if the eigenvalues λ are negative, and hence the system will become unstable [43]. On the other hand, if the eigenvalues λ are positive, then, the perturbation will decay to zero, as $t \rightarrow \infty$, and hence, the system is asymptotically stable.

To reduce the problem to the standard form, we introduce a new transformation

$$\theta(\zeta) = w(\zeta)e^{-\frac{1}{2}v\zeta} \quad (3.18)$$

so that the above eigenvalue problem reduces to the form

$$\frac{d^2w}{d\zeta^2} + [\lambda - q(\zeta)]w = 0, \quad (3.19)$$

where

$$q(\zeta) = \frac{v^2}{2} - (1 - 2\Phi) \geq 2\Phi(\zeta) > 0 \quad \text{for} \quad v \geq 2. \quad (3.20)$$

This is a standard eigenvalue problem, and eigenvalues are real and positive provided $v \geq 2$. This means that all small perturbations of finite extent decay exponentially to zero, as $t \rightarrow \infty$. We conclude that the traveling wave solution of the Fisher equation is asymptotically stable. However, the present perturbation analysis is not completely general. The general problem has been studied by several authors including, for example ref [47].

3.4 Numerical computation of reaction diffusion equation

In this section, we present simulation data for fronts in the nonlinear diffusion equation (3.3) and compare these with our analytical predictions. As an initial condition, we

constant speed.

If we perturb the initial condition by ζ so it becomes

$$\phi(x, 0) = \frac{\zeta}{2} [1 - \tanh(\xi x)] ; \quad (3.23)$$

we can estimate the time τ it takes reach to unity. In Fig 10, you can see perturbations of order ζ grow exponentially at early times with independent of ζ . Time τ is the time necessary for front perturbations to grow exponentially and reach the steady state value $\phi = 1$. These perturbations grow as $O(1)$, where coarsening begins, in time to be given by

$$\zeta e^{2.485\tau} \approx 1 \quad (3.24)$$

In Fig. 11, we focus on the second feature, namely the displacement of the front. We plot the velocity $v(t)$ of various amplitudes ϕ as a function of t . For comparison, the predicted asymptotic value v_{min} is plotted as a dashed line. One observes, that for fixed t , the velocity $v(t)$ is smaller, the larger ϕ is. This is an immediate consequence of the front becoming flatter in time.

In Fig. 8, front propagation speed is plotted as a function of the asymptotic decay rate ξ . The dashed portion correspond to a value of ξ obtained by a linear analysis and solid points corresponds to the numerical simulation of the nonlinear diffusion equation. The straight line marks the values v_{min} .

In Fig. 12, we study the relaxation behavior of front velocity as time $t \rightarrow \infty$. The velocity of the front relaxes like $v(t) = v^* - \frac{6}{5t}$, where v^* is the asymptotic speed of the front.

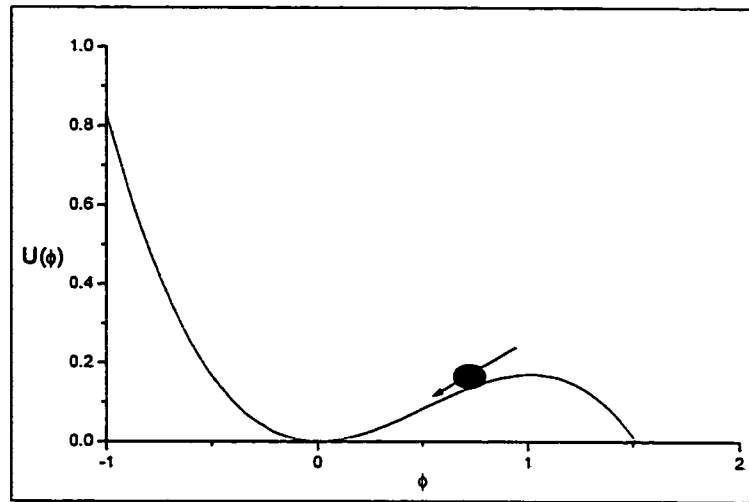


Figure 7: Potential $U(\phi) = \frac{1}{2}\phi^2 - \frac{1}{3}\phi^3$. Equation (3.4) for a profile moving with steady state velocity v can be interpreted as the equation for a particle subject to friction moving down the potential.

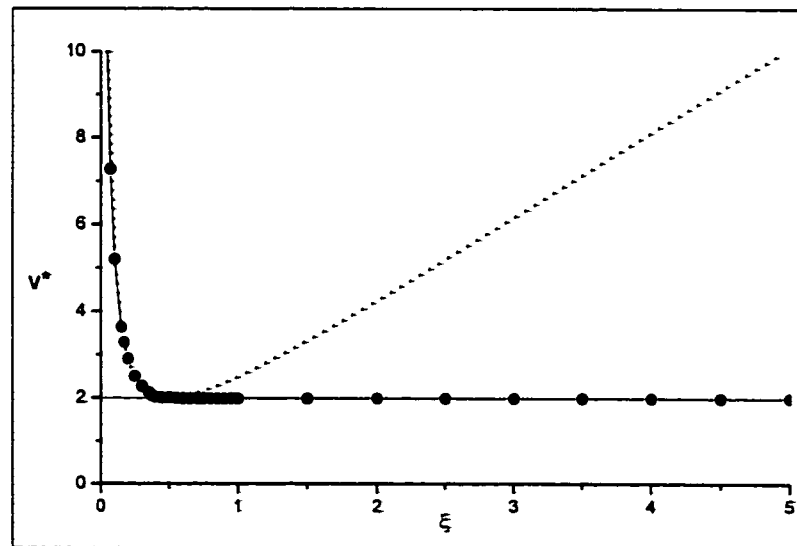


Figure 8: Velocity against ξ . The solid line is the numerical simulation and the dotted line is the theoretical value.

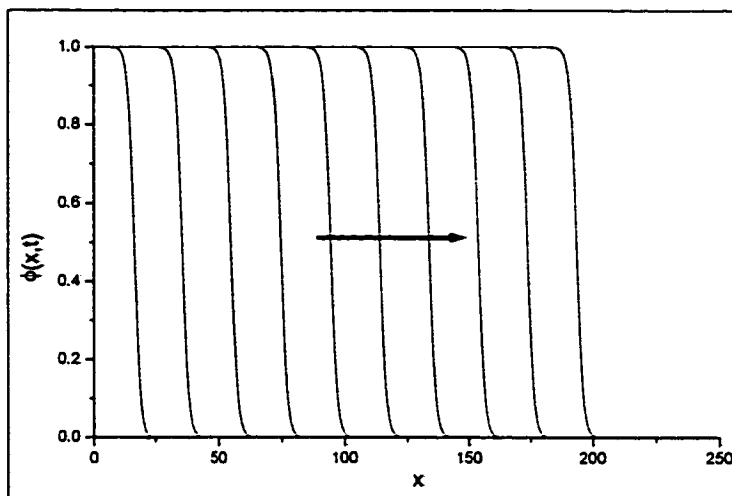


Figure 9: Shape of the front at different times.

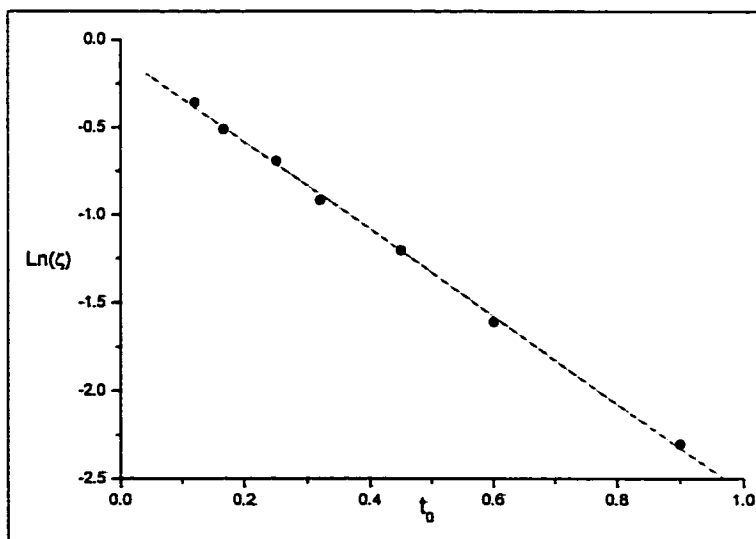


Figure 10: $\text{Ln}(\zeta)$ as function of time to reach the unity

CHAPTER 4

Noise effect on front propagation

The study of the effects of fluctuations on front propagation under nonequilibrium conditions [10] constitutes an active field of research both experimentally [48] and theoretically [49]. The amplification of fluctuations seems to be an important ingredient in the explanation of phenomena such as instabilities in Rayleigh-Benard convection [50] and Taylor-Couette flow [49]. Nevertheless, a theoretical framework which includes the effects of fluctuations on instability dynamics is only starting to be developed. Moreover, there has been some theoretical work on external noise effect in spatially extended systems [51] in the hope to explain the discrepancies between the experimental and theoretical results. It has been predicted the existence of a shift in the transition point of the Swift-Hohenberg [52] and Ginzburg-Landau models [52] caused by noise.

Both analytical and numerical work have been carried out to explain such phenomena [53]. However, many fundamental aspects such as the origin of the noise [54], or the correct modeling of the coupling between the noise and the state of the system [55] remain to be clarified. Generally, noise can affect the phenomenological description of a reaction-diffusion system in various ways. A first possibility is intrinsic noise modelled typically

by additive thermal noise in a Langevin type equation. A second possibility is the external noise, e.g., due to fluctuations of a control parameter. This is known as multiplicative noise. Its effects on the system are, in general, more important than those induced by a simple additive noise. The reason is that the existence of a coupling could induce amplification of the stochastic effect. In some experiments in liquid crystals [56], this situation has been studied by deliberately superimposing a noise to the ac voltage. This results in a strong effect on the response of the system, that changes the threshold of the instability points.

Theoretical studies of the effects of multiplicative noise have been carried out in simple models without spatial dependence [57]. But very little is known regarding spatially extended systems. Some aspects need to be studied in detail, like the interpretation of the stochastic equations or the analytical and even the numerical treatment of the equations. To this end, in this chapter we start by introducing additive noise on reaction diffusion equation and then study the effect of external noise on front propagation. The resulting equation with multiplicative noise could be used to describe the temporal evolution of the concentrations of a system of two components, like a binary liquid or an alloy that could undergo phase separation [57]. In this situation, the system is suddenly quenched from a one-phase region inside its coexistence region. Then, the homogeneous phase becomes unstable and domains of the new stable phases start growing.

4.1 Internal Noise

The study of the role of additive noise on the propagation of fronts into unstable media

was addressed few years ago in ref [58] . The effects of nonzero temperature fluctuations can be analyzed by means of the following dimensionless dynamical model:

$$\frac{\partial \phi}{\partial t} = \frac{\partial^2 \phi}{\partial x^2} + f(\phi) + \eta(t) \quad (4.1)$$

with $f(\phi) = \phi(1-\phi)(1-a\phi)$ as a general model, where a is a control parameter and where $\eta(t)$ is assumed to be a Gaussian white noise of zero mean and correlation,

$$\langle \eta(t_1)\eta(t_2) \rangle = 2\epsilon \delta(t_1 - t_2) . \quad (4.2)$$

In this way, the noise strength parameter ϵ is a dimensionless measure of temperature. We have numerically solved (4.1) under appropriate initial conditions by introducing a quantity $x_0(t)$ defined as

$$\langle \phi(x_0(t), t) \rangle = \frac{1}{2}, \quad (4.3)$$

which we identify as the position of the front. The brackets denote the average over the noise field. The velocity of propagation of the front can be defined as

$$v(t) = \frac{dx_0(t)}{dt}. \quad (4.4)$$

We consider front propagation described by this equation under initial conditions given by (3.21).

In Fig. 13, we consider first the case of a moderate noise level $\epsilon = 0.001$. We show the function $\langle \phi(x_0(t), t) \rangle$ at five equally spaced times between $t = 10$ and $t = 100$. It is apparent from the figure that while the front propagates, its velocity decreases with time. To investigate this decrease in a quantitative way we take recourse to the quantity $x_0(t)$ introduced in the preceding section. This quantity, as extracted from the data shown in Fig. 13, is plotted in Fig. 14 as a function $t^{1/2}$. The line plotted is a best fit to the form $x_0(t) = 0.543t^{1/2} + 4.244$. Thus, we have a clear indication that the size of the front position increases as $t^{1/2}$, at least for $t > 10$. In other words, the front propagation velocity decrease with time as $t^{-1/2}$.

We have obtained results for different noise levels over a finer time mesh, including earliest times. An illustrative subset of the results for $\langle \phi(x_0(t), t) \rangle$ versus x_0 is displayed in Fig. 15. One can see in these figures, that front slows down. We have analyzed our results at these noise levels in terms of $x_0(t)$. The results are plotted in Fig. 16 as a function of $t^{1/2}$. The results for $\epsilon = 0$ are also indicated. For sufficiently early times the behavior of $x_0(t)$ tracks precisely the zero noise curve, which is approximately a parabola in the plot. At a certain characteristic time t_0 which increases slowly as the noise strength decreases, the curve for $x_0(t)$ breaks off the zero noise strength curve and abruptly switches to the $t^{1/2}$ behavior, which is a straight line in the plot. The slope of the straight line decreases somewhat with ϵ .

In Fig. 17, We displayed t_0 as function of ϵ . Thus, we expect the crossover time t_0 to

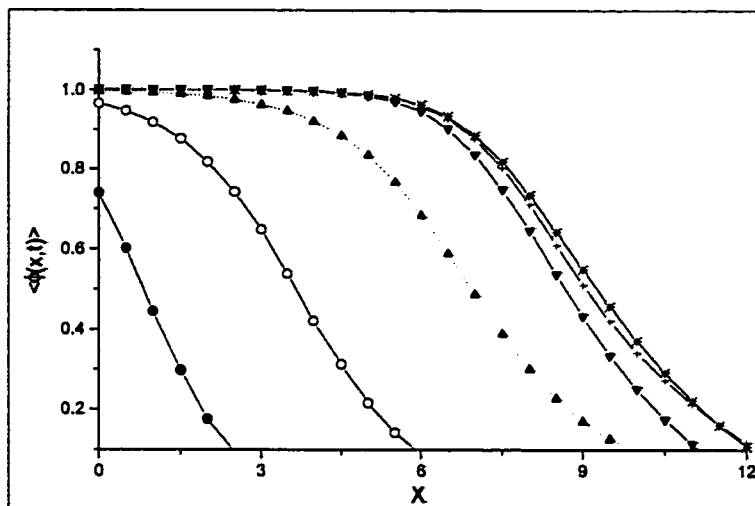


Figure 13: Front propagation with internal noise and with intensity $\epsilon = 0.001$, we show the function $\langle \phi(x_0(t), t) \rangle$ at five equally spaced times between $t = 10$ to $t = 100$. Symbols are indicate eyes

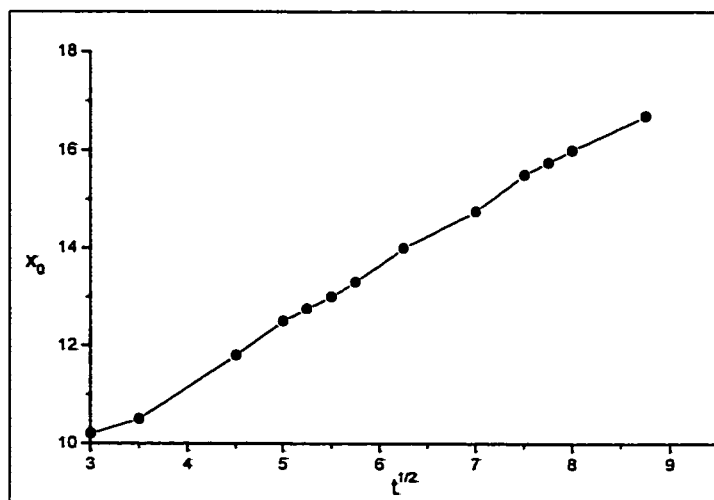


Figure 14: The quantity x_0 obtained from the data in Fig.13 as function of $t^{1/2}$.

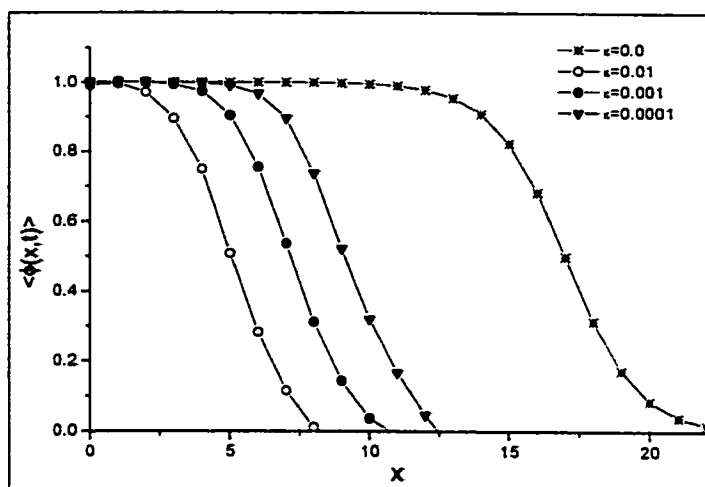


Figure 15: Numerical results for $\langle \phi(x, t) \rangle$ at different noise intensity ϵ and a fixed value of time $t = 50$.

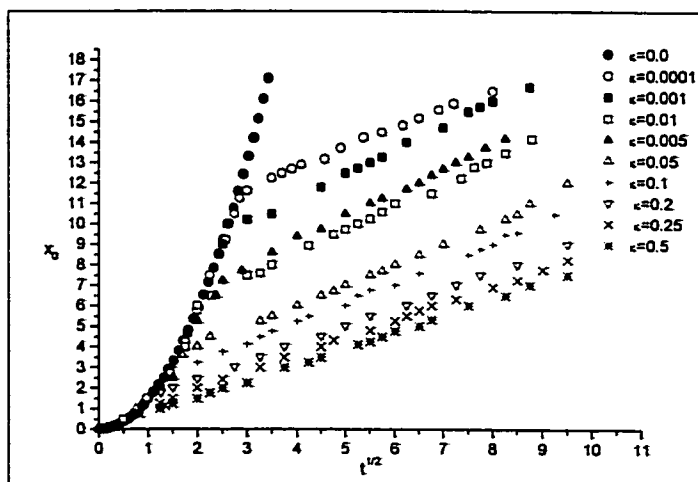


Figure 16: Results for x_0 at very low noise levels, extracted from data shown in Fig.13

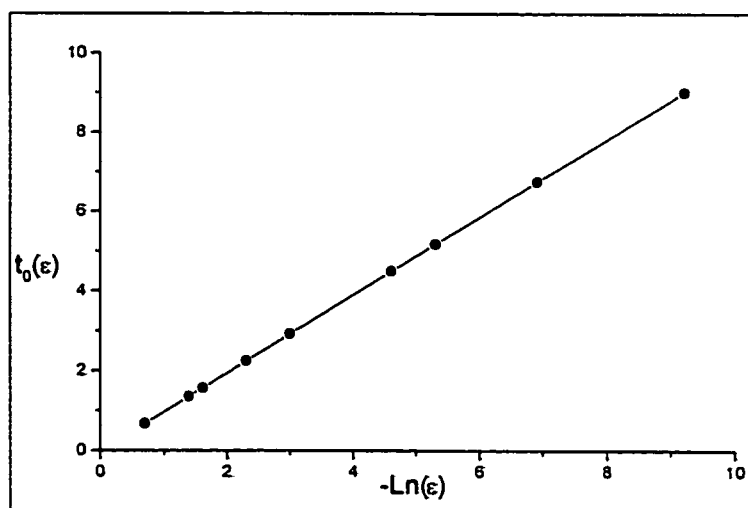


Figure 17: Characteristic time t_0 as function of noise intensity $-\ln(\epsilon)$, extracted from Fig.16.

fluctuations can be due to a fluctuating environment or can be the result of an externally applied random force. The mathematical modeling of this fluctuation is made by considering a deterministic equation appropriate in the absence of external fluctuations [60]. One then considers the external parameter which undergoes fluctuations to be a stochastic variable. The noise term of the stochastic differential equation obtained in this way is usually of multiplicative character; that is, it depends of the instantaneous value of the variables of this system. It does not scale with system size and is not necessarily small comparable to unity. We can regard the external noise as fluctuations in an external field which drives the system. Several experimental situations in the presence of external noise have been recently considered. These include illuminated chemical reactions [10], electric circuits [59] and electrohydrodynamic instability in liquid crystals [10].

It is known that the presence of noise can stabilize a system that is otherwise unstable. On the other hand, one has the intuitive idea that a strong enough noise would destroy the order present in a system. It then seems necessary to study systematically the possible effects of external noise on a system. Indeed, in some of the experimental situations mentioned above, it has been observed that the threshold value for which the system undergoes a nonequilibrium transition depends on the noise parameters, so that it can be modified by varying, say, the noise intensity.

Our starting point is the following generic nonlinear diffusion equation

$$\frac{\partial \phi}{\partial t} = \frac{\partial^2 \phi}{\partial x^2} + f(\phi, \alpha), \quad (4.7)$$

trative simulation of the Eq.(4.9) shown such as Fig. 18. We have used a standard finite-difference Euler algorithm with spatial mesh size Δx and time step Δt adequate to ensure stability and accuracy (see Appendix A).

As shown in Fig. 18, for moderate noise intensities one sees that the front has a rather well defined position and width, and basically a kink-like shape which is not destroyed by noise. The position of the front can thus be defined by the integral $x(t) = \int dx\phi(x, t)$. The instantaneous front velocity for a particular realization is then obtained as $v = \frac{dx(t)}{dt}$, and then averaged over an appropriate number of realizations to eliminate statistical fluctuations. In Fig. 18 it is also apparent that the noisy front gets faster as the intensity of noise increases.

We will now make use of numerical simulations to evaluate the propagation velocity of a one-dimensional fluctuating front. Fig. 19, shows the mean propagation velocity obtained from numerical integration of the stochastic front model defined by equation (4.9) as a function of time. As expected from Fig. 20, the functional dependence of the front speed on the effective noise intensity ϵ increases almost linearly. In Fig. 21, we measure the width of front for long time with noise strength $\epsilon = 0.5$. The width will go to a constant value for long times. Therefore, we measure the width for long time with different noise strengths. The width of the front increases as the noise strength increases as shown in Fig. 22.

In Fig. 23, we also find the relaxation time of the velocity with noise. As we can see from Fig. 23, the speed relaxes as $v(t) \approx v^* - \frac{(1.217+2.485\epsilon)}{t}$, where v^* is the asymptotic speed of the front with noise and its depends on noise intensity. This mean that the relaxation time depends on intensity of noise.

To sum up, the internal noise slows down the motion of the front and causes a crossover

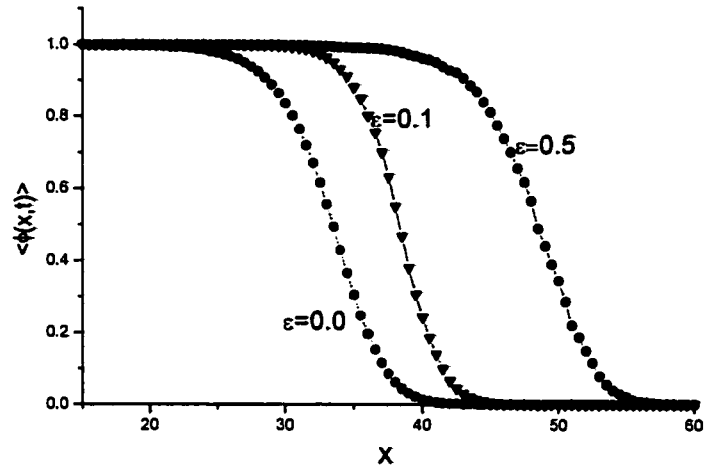


Figure 18: Front propagation shape as function of space with different external noise intensity ϵ and a fixed value of time $t = 100$.

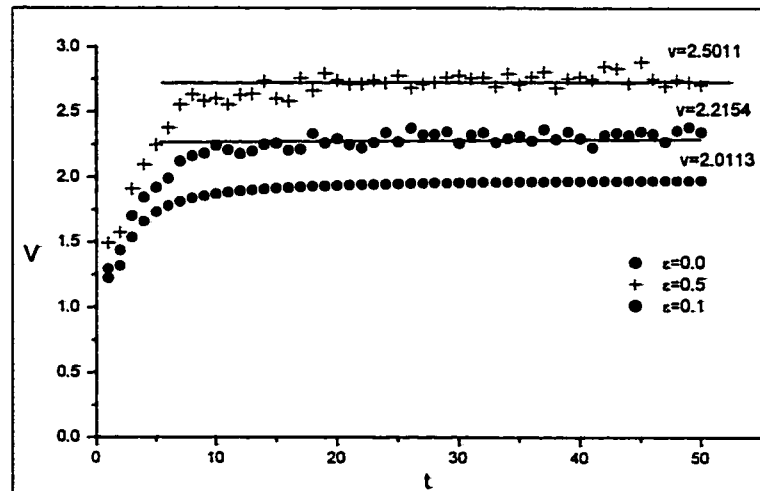


Figure 19: Front velocity vs time for several values of noise intensity ϵ .

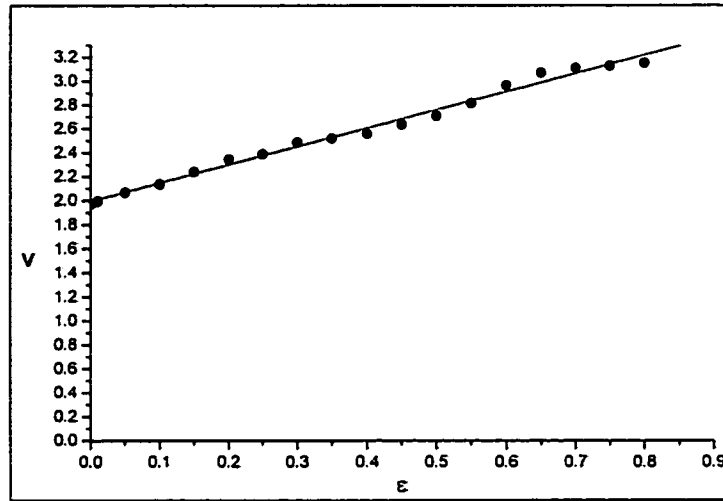


Figure 20: Front velocities vs noise intensity ϵ . The symbol represent the numerical results. The straight line is a least squares linear fit of v vs ϵ .

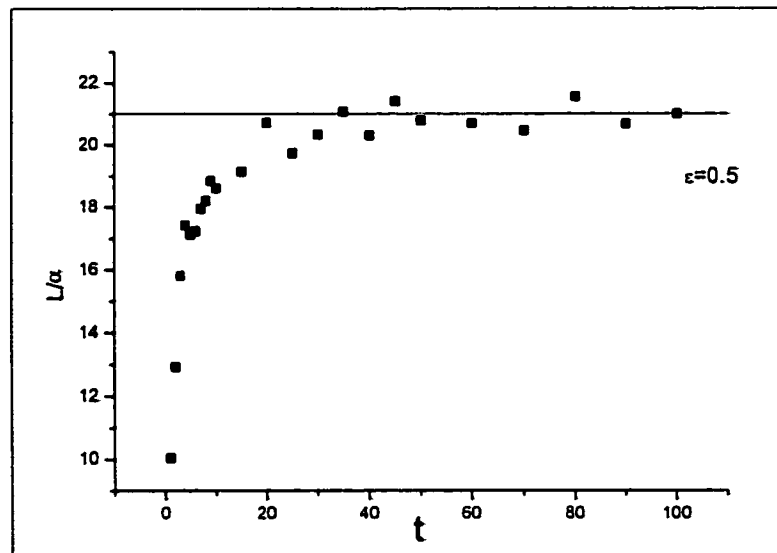


Figure 21: Width of the front as function of time when the noise strength is 0.5.

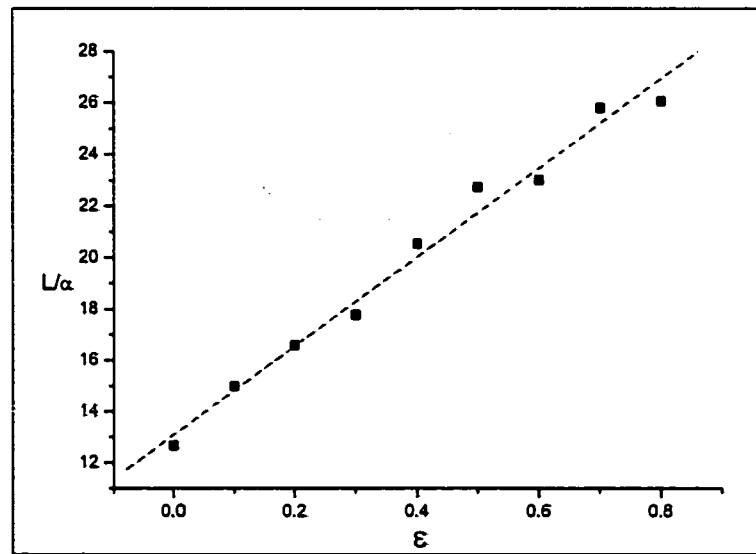


Figure 22: Width of the front propagation as function noise intensity.

from ballistic behavior at early times to diffusive behavior at late times. In fact, in the presence of internal noise, the front itself exists only for a short transient. External noise, on the other hand, increases the mean propagation velocity of the front linearly with noise intensity. In addition, the width of the front increases as the external noise strength of increases.

CHAPTER 5

Disorder effect on Front Propagation

Wave propagation through nonlinear systems having localized impurities (or defects) is a fundamental problem in solid state physics [67]. Impurities break the translational symmetry of a physical system and lead to several effects such as wave reflection, resonant scattering excitation of impurity modes and spatially localized oscillatory states at the impurity sites [68]. These two kinds of problems, i.e., wave propagation in inhomogeneous media and defect supported localized modes, appear in many different physical problems, such as the scattering of surface acoustic waves by surface defects or interfaces [69], the dynamics of the tight binding Holstien-type models of the electron phonon coupling [70], light propagation in dielectric superlattices with embedded defect layers [71], etc. In all such cases, the impurities (or defects) lead to energy trapping and localization in the vicinity of the defects. They occur in the form of spatially localized impurity modes.

When nonlinearity becomes important, it may lead to self-trapping and energy localization even in a perfect (or homogeneous) system in the form of intrinsic localized modes. Spatially localized modes of nonlinear systems are usually associated with solitary waves

(or solitons) in continuous models; or discrete breathers in lattice models; and they have been a subject of intensive studies during the past few years [72]. However, the study of nonlinear phenomena in inhomogeneous and disordered systems is still largely an open area of research [73]. Simultaneous presence of nonlinearity and disorder is associated with various dynamical processes in solids, biological systems, and optics [75]. For example, nonlinearities can become important even in a harmonic lattice due to the interaction of an exciton with the lattice vibrations [74], where impurities may appear as a result of doping of materials with atoms or molecules that have stronger local coupling. Such impurities can also appear in spin wave systems due to, e.g. a local variations of the coupling between neighboring spins [75].

When both nonlinearity and disorder are present simultaneously, it is expected that competition between two different mechanisms of energy localization (i.e. one due to the self-action of nonlinearity, and the other one, due to localization induced by disorder) will lead to a complicated and somewhat nontrivial physical picture of localized states and their stability. In this chapter, we study the static properties of disordered front propagation models where the disorder is assumed to be a δ -correlated Gaussian spatial noise. The disorder of this kind is akin, for example, to Josephson junctions, where it is caused by the fluctuations of the gap between two superconductor plates.

Model and Numerical results

Let us consider a front propagating in a nonlinear system in the presence of static impurities. To be specific, and to make calculations simpler, let us choose the nonlinear diffusion equation model as a particular realization of this problem, described by the following equation for the wave field $\phi(x, t)$:

$$\frac{\partial \phi(x, t)}{\partial t} = \frac{\partial^2 \phi(x, t)}{\partial x^2} + f(\phi) + \epsilon(x)\phi \quad (5.1)$$

where $f(\phi) = \phi(1 - \phi)(1 - a\phi)$ (For simplicity we choose $a = -1$). In the simplest model of a disordered system, the function $\epsilon(x)$ may be taken as a sum of δ functions,

$$\epsilon(x) = \beta \sum_n \delta(x - x_n) \quad (5.2)$$

and describes random-point impurities with equal intensities β and at random positions x_n , and it may represent, e.g., the structural disorder of the associated system. We solve Eq. (5.1) by using Euler method as described in chapter 3 (See Eq. (3.22)) with number of realization 5000.

We introduce a local impurity at position $x = 565$ in the system with intensity $\beta = 0.5$ (Where $\beta \geq 0$ corresponds to an attractive potential and $\beta < 0$ to a repulsive potential) .As shown in Fig. 24, after the front passes over an impurity, it recovers its original speed, and the only permanent change in it is a phase shift and give rise to a small distortion that is localized in the vicinity of the impurity and which lise to a slight modification in its shape

as in reference [76].

In Fig. 25 and 26, the impurities are introduced in the system with concentration of 5% at random positions. As we can see from these figures, some modification to the front is observed. The amplitude of the front (A), velocity (v) and the width of the front (L) are changed. In Fig. 27, the velocity is changed linearly with intensity of impurity where the velocity is increased as the intensity increased. Also, the amplitude of the front increase linearly with respect to intensity as shown in Fig. 28. However, in Fig. 29, the width of the front decreases linearly. We increase the concentration of the disorder in the system and fix the intensity to $\beta = 0.1$. The simulations show that the velocity, amplitude and the width are changed linearly when the concentration is increased.

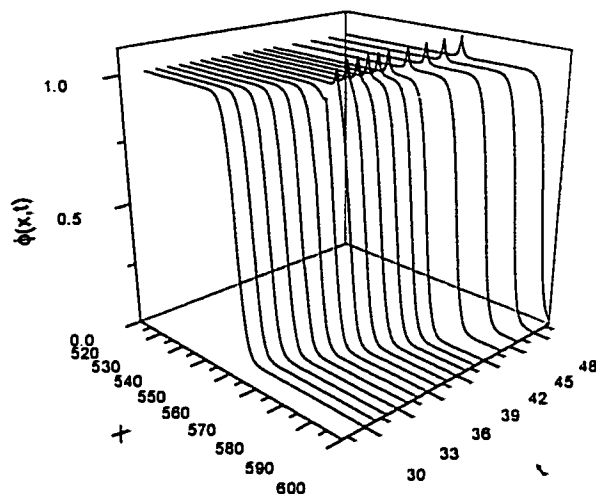


Figure 24: Front propagation when a single impurity whose strength is 0.5 at $x = 565$.

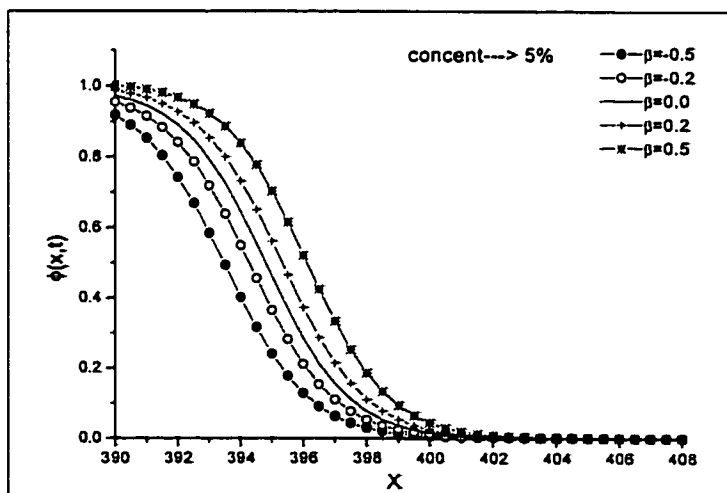


Figure 25: Front propagation as function of space with different external disorder intensity β . The concentration of disorder impurities is 5%.

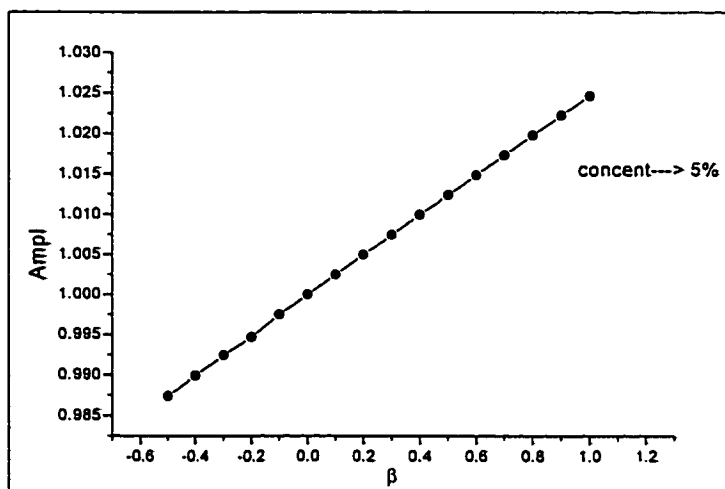


Figure 28: Amplitude of the front propagation as function of disorder intensity β . The concentration of impurities is fixed to 5% at $t = 100$.

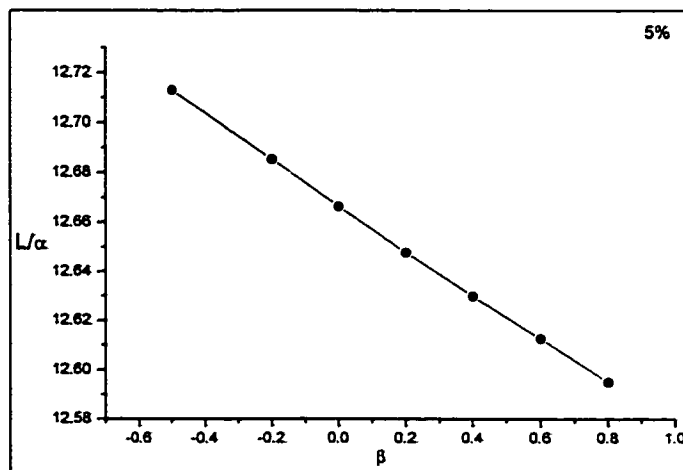


Figure 29: Width of the front propagation as function of disorder intensity β . The concentration of impurities is fixed to 5% at $t = 100$.

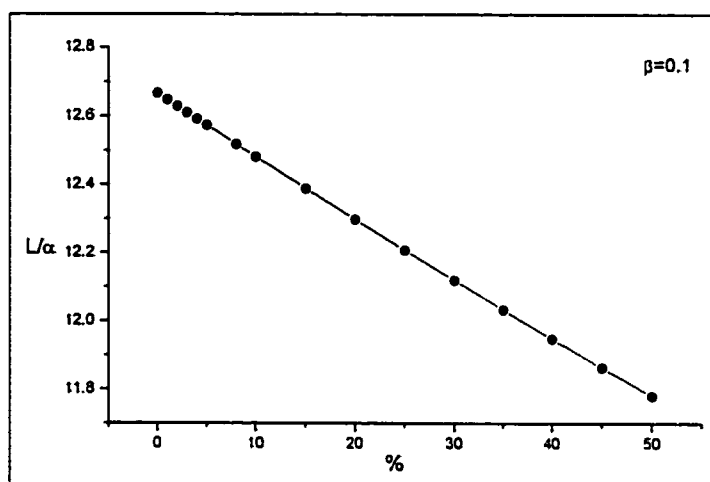


Figure 32: Width of the front propagation as a function of impurity concentration. The intensity of impurity potential is 0.1.

CHAPTER 6

Conclusion

In this thesis, we studied different aspects of noise and disorder effects on front propagation in nonlinear media. From Langevin equation we have checked how fluctuation affects the motion of a particle as a function of time and we have found that the noise changes the behaviour of the mean square displacement for long times. We study the front propagation numerically and analytically, where the velocity of the front go to asymptotic value for long time. We investigate the perturbation of initial condition and found that the time grow exponentially and reach the steady state value. We showed that the properties of the front propagation exhibit strong dependence on the noise intensity. When the noise is internal, the intensity of noise slows the front motion.. Moreover, the internal noise would trigger the formation of domains of two phases, modifying the nature of the problem into a phase separation process with diffusive dynamics. In this case, the front itself exists only during a short transient. We introduce the noise through the fluctuations of a control parameter which leads to a multiplicative (external noise) stochastic partial differential equation. The effects of external fluctuations in front propagation, provided they enter multiplicatively in the equations, are twofold: first, they induce a shift in the mean front shape, and second,

the mean velocity increases linearly with the noise intensity. Also, the width of the front increases proportional to the noise intensity. We have investigated numerically the problem of front propagation through a disordered medium, where disorder was modeled by δ -like impurities with equal intensities but random positions. We have checked how the mean velocity, the amplitude and the width evolve with time, and we have concluded that the velocity is linearly proportional to the strength of the disorder. Also, the amplitude of the front is increased proportional to the strength of disorder. However, the width of front is inversely proportional to the disorder strength.

There are many open questions remain to be answered. Concerning the simulation of stochastic partial differential equation can be considered to have reached their maturity, and probably only some minor improvements are to be expected, mainly in the direction of increasing the speed and reducing the statistical errors of the algorithms. On the other hand, the generation of noises with prescribed statistical properties mimicking real noises is open for drastic improvements. Within the particular problems that have been addressed here, some unsolved questions remain to be clarified.. The study of the influences of structured (colored) noises deserves more attention. Another topic that still needs to be satisfactorily faced is the analysis of noise effects in two dimensional fronts.

Along with the previously mentioned fundamental developments, many particular applications are suitable for analyzing, both theoretically and experimentally, the nontrivial influence of noise in front systems. We now list a few potential subjects of study [10], some of which are already under investigation by different research groups:

- Much interest is aroused these days by the dynamical behavior of front propagation.

Fields such as biophysics and chemistry are currently witnessing interesting and important developments in this direction.

- Hydrodynamic systems in the presence of noise are particularly difficult to study, and probably drastic simplifications will have to be implemented if external noise to be taken into account.
- Finally, much work is still required in nonlinear optical systems, where effects of external fluctuations in the transverse instabilities induced by light diffraction is a completely open subject.

The previous list does not aim to be exhaustive, but it is provided as an example of the huge variety of open problems where the presence of either unavoidable (internal noise) or externally imposed sources of noise can lead to nontrivial phenomena.

APPENDIX A: Stability of Reaction Diffusion Equation

The classical example of the parabolic equation is the diffusion equation

$$\frac{\partial u}{\partial t} - D \frac{\partial^2 u}{\partial x^2} = 0 \quad (\text{A-1})$$

As a first attempt to solve (A-1), we consider either using centered second order differences for the space derivative and Euler's method for the time part

$$u_j^{n+1} = u_j^n + \frac{D\delta t}{\delta x^2} (u_{j+1}^n - 2u_j^n + u_{j-1}^n) \quad (\text{A-2})$$

where the subscripts j represent space steps and the superscripts n represent time steps. The stability is a property of the time, t , integration rather than the space, x . We analyze this by considering a plane wave solution for the x -dependence by substituting $u_j^n = v^n \exp(ikx_j)$ to obtain

$$v^{n+1} e^{ikx_j} = v^n e^{ikx_j} + \frac{D\delta t}{\delta x^2} v^n (e^{ikx_{j+1}} - 2e^{ikx_j} + e^{ikx_{j-1}}) \quad (\text{A-3})$$

or, after dividing out the common exponential factor,

$$v^{n+1} = v^n \left[1 - \frac{4D\delta t}{\delta x^2} \sin^2 \left(\frac{D\delta x}{2} \right) \right] \quad (\text{A-4})$$

Hence, the stability condition is simply given by the quantity in square brackets. The condition that the method is stable for all D gives

$$\delta t \leq \frac{1}{2} \frac{\delta^2 x}{D} \quad (\text{A-5})$$

This is known as the *von Neumann* stability condition.

REFERENCES

1. R. E. Goldstein, D. J. Muraki and D. M. Petrich, *Phys. Rev. E* **53**, 3933 (1996).
2. P. W. Bates, P. C. Fife, R. A. Gardner and c. K. R. T. Jones, *Physica D* **104**, 1 (1997).
3. J. S. Langer, *Rev. Mod. Phys.* **52**, 1 (1980).
4. C. Livermore and P. Wong, *Phys. Rev. Lett.* **72**, 3847 (1994).
5. J. B. Swift and P. C. Hohenberg, *Phys. Rev. A* **46**, 4773 (1992).
6. D. Bensimon, L. P. Kadanof, S. Liang, B. I. Schraiman, and CH. Tang, *Rev. Mod. Phys.* **58**, 977 (1986).
7. E. Brener, T. Ihle, H. Muller-Krumbhaa, Y. Saito, and K. Shiraishi, *Physica A* **204**, 96 (1994).
8. L. M. Williams, M. Muschol, X. Qian, and H. Z. cummins, *Phys. Rev. E* **48**, 489 (1993).
9. K. Huang; *Statistical Mechanics*; Wiley Press, 1987.
10. M.C. Cross and P.C. Hohenberg, *Rev. Mod. Phys.* **65**, 851 (1993).
11. R. K. Pathria; *Statistical Mechanics*; Pergamon Press, 1972.
12. R. Kubo; *Science* **233**, 330 (1986).
13. D. T. Gillespie; *Am. J. Phys.* **61**, 1077 (1993).
14. T. Srokwski and M. Ploszajczak; *Phys. Rev. E* **57**, 3829 (1997).
15. D. Gillespie; *Phys. Rev. E* **54**, 2084 (1996).
16. A. Lemarchand, A. Lesne and M. Mareshcal; *Phys. Rev. E* **51**, 4457 (1995).
17. D. T. Gillespie; *J. Appl. Phys.* **83**, 3118 (1998).
18. F. Mandl; *Statistical Physics*; Wiley Press, 1988.
19. M. Ploszajczak and T. Srokwski; *Anna. Phys.* **249**, 236 (1996).

20. D. T. Gillespie; *Am. J. Phys.* **64**, 225 (1996).
21. A. Manoliv and C. Kittel; *Am. J. Phys.* **47**, 678 (1979).
22. A. C. Branka and D. M. Heyes; *Phys. Rev. E* **58**, 2611(1998).
23. N. J. Rao, J. D. Borwankar, and D. Ramkrishna; *SIAM J. Control* **2**, 295 (1974).
24. R. Mannella and V. Palleshi; *Phys. Rev. A* **40**, 3381 (1989).
25. R. L. Honeycutt, *Phys. Rev. A* **45**, 600 (1992).
26. R. L. Honeycutt, *Phys. Rev. A* **45**, 604 (1992).
27. R. F. Fox, I. R. Gatland, R. Roy, and G. Vemuri; *Phys. Rev. A* **38**, 5938 (1988).
28. R. F. Fox; *Phys. Rev. A* **43**, 2649 (1991).
29. F. James, *Comput. Phys. Commun.* **60**, 329 (1990).
30. W. H. Press, S. A. Teukolsky, W. T. Vetterling and B. P. Flannery, *Numerical Recipes*, Cambridge University Press 1992.
31. A. Lemarchand, B. Nowakowski; *J. Chem. Phys.* **111**, 6190 (1999).
32. D. Vives, A. Careta and F. Sagués, *J. Chem. Phys.* **107**, 7894 (1997).
33. A. R. Kerstein, W. T. Ashurst, and F. A. Williams, *Phys. Rev. A* **37**, 2728 (1988).
34. J. D. Murray, *Mathematical Biology*, Springer-Verlag, Berlin, 1989.
35. R. A. Fisher, *Ann. Eugenics* **7**, 355 (1937).
36. J. Riordan, C. R. Doering and D. ben-Avranham; *Phys. Rev. Lett* **75**, 565 (1995).
37. D. A. Kessler and Z. Ner; *Phys. Rev. E* **58**, 107(1998).
38. G. Dee and J. S. Langer; *Phys. Rev. Lett.* **50**, 383 (1983).
39. W. Van Saarloos; *Phys. Rev A* **37**, 211 (1988).
40. W. Van Saarloos; *Phys. Rev A* **39**, 6367 (1989).
41. E. Ben-Jacob et al; *Physica D* **14**, 348 (1985).
42. W. Van Saarloos; *Phys. Rev. Lett.* **58**, 2571 (1987).

43. F. Brauer and J. A. Nohel; *The Qualitative Theory of Ordinary Differential equations* ,Dover Publications , 1969.
44. R. Gallego, M. San Miguel and R. Toral; Phys. Rev. E **58**, 3125 (1998).
45. U. Ebert and W. Van Saarloos; e-print cond-Matt/0003181.
46. P. Collet; *Instabilities and Fronts in Extended Systems*, Princeton University Press, 1990.
47. Ute Ebert, and Wim van Saarloos, cond-mat/0003181.
48. C.Livermore and P. Wong, Phys. Rev. Lett. **72**, 3847 (1994).
49. J. B. Swift, K. L. Babcock, and P. C. Hohenberg, Physica A **204**, 625 (1994).
50. P. C. Hohenberg and J. B. Swift, Phys. Rev. A **46**, 4773 (1992).
51. C. Van den Broeck, J. M. Parrondo, J. Armero, and A Hernandez-Machado, Phys. Rev. E **49**, 2639 (1994).
52. A. Becker and L. Kramer, Phys. Rev. Lett. **73**, 3395 (1994).
53. M.J. Gingras and Z. Racz, Phys. Rev. A **40**, 5960 (1989).
54. W. Meyer, G. Ahlers, and D. Cannell, Phys. Rev. A **44**, 2514 (1991).
55. R. Pieterss, Phys. Rev. A **37**, 3126 (1988).
56. W. van Saarloos, M. Van Hecke, and R. Holyst, Phys. Rev. E **52**, 1773 (1995).
57. W. Horsthemke and R. Lefever, Noise-induced transtions (Springer, Berline, 1984).
58. O. T. Valls and L. M. Lust, Phys. Rev. B **44**, 4326 (1991).
59. S. Kabashima, S. Kogura, T. Kawakubo and T. Okada, J. Appl. Phys. **50**, 6296 (1979).
60. A. H. Romero and J. M Sancho; Phys. Rev E **58**, 2833 (1998).
61. D. T. Gillespie; J. Chem. Phys. **113**, 297(2000)
62. A. Greiner, W. Strittmatter and J. Honerkamp; J. Stat. Phys. **51**, 95 (1988)
63. A. M. Jayannavar; Phys. Rev. E **48**, 837 (1993)
64. I. Sendia-Nadal and et al.; Phys. Rev. Lett. **84**, 2734 (2000)

65. A. C. Branka and D. M. Heyes; *Phys. Rev E* **58**, 2611 (1998)
66. K. K. Manne, A. J. Hurd and V. M. Kenkve; *Phys. Rev. E* **61**, 4177 (2000)
67. A. L. Efros and M. Pollak, *Electron-Electron Interaction in disordered Systems* (North Holland, Amsterdam, 1986).
68. Yu. S. Kivshar and S. A. Gredeskul; *Phys. Rev. Lett.* **64**, 1693 (1990).
69. Ping Sheng, *Scattering and Localization of classical Waves*, World Scientific, 1990.
70. M. I. Molina and g. P. Tsironis, *Phys. Rev. B* **47**, 15 330 (1993).
71. E. Lidorikis, K. Bush, Q. Li, C. T. Chan, and c. M. Soukoulis, *Phys. Rev. B* **56**, 15 090 (1997).
72. S. Flach and C. R. Willis, *Phys. Rep.* **295**, 181 (1998).
73. S. A. Gredeskul and Yu. S. Kivshar, *Phys. Rep.* **216**, 1 (1992).
74. V. M. Kenkre and D. K. Campbell, *Phys. Rev. B* **34**, 4959 (1986).
75. W. J. Tomlinson, *Opt. Lett.* **5**,323 (1980).
76. B. A. Malomed, *Physica D* **15**, 385 (1985).

APPENDIX

UNCERTAINTY AND ERROR ANALYSIS

1. Direct Measurements (Independent variables)

Direct Measurements	Measured by	Accuracy
Dry Bulb temperature	Thermocouple	$\pm 0.1^{\circ}C$
Wet Bulb temperature	Thermocouple	$\pm 0.1^{\circ}C$
Pressure	Pressure gauge	$\pm 1 \text{ psi}$
Flow rate (1)	Flow meter	$\pm 25 \text{ l/h}$
Flow rate (2)	Flow meter	$\pm 1 \text{ l/min}$
Electric power	Power meter	$\pm 0.1 \text{ kW h}$
Relative humidity	VelociCalc instrument	$\pm 0.1 \%$
Specific gravity (and hence concentration)	Hydrometer	± 0.02
	Which corresponds to concentration difference of	± 0.1

2. Dependent Variables

Variables	e_{\max}	e_{\min}	% Uncertainty	
			Max.	Min.
Effectiveness (ξ)	0.0168	0.009148	0.061	0.058
Outlet & inlet humidity ratio (ω_o/ω_i)	0.0218	0.1029	2	3.76

References:

- [1] "Electricity growth and development in the Kingdom of Saudi Arabia up to year 1412H (1992G)", Studies and Statistics, Ministry of Industry, Kingdom of Saudi Arabia, 1412H (1993G).
- [2] J. Marsala et al., "Liquid desiccant for residential applications", ASHRAE Trans., 95, 1, 828-834, 1989.
- [3] G.O.G., Lof, "House heating and cooling with solar energy". In Solar Energy Research, University of Wisconsin Press, 33-46, 1955.
- [4] P. Gandhidasan, and M.C. Gupta, "A new method of sun powered air-conditioning". Bull. I.I.R. Annex 1976-1, 665-672, 1976.
- [5] H. I. Robison, Open cycle chemical heat pump and energy storage system. Final Report for Solar Energy Research Institute, Coastal Carolina Energy Laboratory of University of South Carolina, Conway, Sub-contract No. ZE-0-9185-1, Jan. 1982.
- [6] S. Jain, P. L. Dhar, and S.C. Kaushik, " Evaluation of liquid desiccant based evaporative cooling cycles for typical hot and humid climates". Heat Recovery Systems & CHP, 14, 6, 621-632, 1994.
- [7] B. Kovak, P.R. Heimann, and J. Hammel, "Sanitizing effects of desiccant-based cooling", ASHRAE Journal, 39, 4, 60-64, 1997.
- [8] L. G. Harriman, The Dehumidification Handbook. Second edition, Munters Cargocaire, Amesbury, MA, 1990

- [16] Lof, G.O.G, Lenz, T.G., and Rao, S., "Coefficients of heat and mass transfer in a packed bed suitable for solar regeneration of aqueous lithium chloride solutions", *Journal of Solar Energy Engineering*, 106:387-392.
- [17] Oberg, Viktoria Eva. "Heat and mass transfer study of a packed bed absorber/regenerator for solar desiccant cooling (Triethylene glycol, air conditioning)". PhD Dissertation, University of Florida, 1998.
- [18] A. Ertas, P. Gandhidasan, I. Kiris, E.E. Anderson. "Experimental study on the performance of a regeneration tower for various climatic conditions", *Solar Energy*, 53(1):125-130, 1994
- [19] A. Ertas, P. Gandhidasan, I. Kiris, E.E. Anderson and M. Dolan, "Experimental investigation on the performance of a packed bed dehumidifier for various climatic conditions", *General Papers in Heat Transfer and Heat Transfer in Hazardous Waste Processing*, HTD-212, ASME 1992.
- [20] Mc Donald, B, Waugaman, D.G., and Kettleborough, C.F., "A statistical analysis of a packed tower dehumidifier", *Drying Technology*, 10(1):223-237.
- [21] Tsair-Wang Chung. "Dehumidification of air by aqueous lithium chloride in a packed column", *Separation Science and Technology*, 28(1-3):533-550, 1993.
- [22] Tsair-Wang Chung and Honda Wu, "Comparison between spray towers with and without fin coils for air dehumidification using triethylene glycol solutions and development of the mass transfer correlations", *Ind.Eng. Chem.*, 39:2076-2084, 2000.
- [23] Tsair-Wang Chung, "Predictions of moisture removal efficiencies for packed-bed dehumidification systems", *Gas Separation and Purification*, 8(4): 265-268, 1994.

- [24] S.Kavasogullari, P. Gandidasan, A.Ertas, and E. E. Anderson. "Performance of CaCl_2 and LiCl and liquid desiccants in a dehumidifying packed tower", *Emerging Energy Technology*, ASME, 36:45-49, 1991.
- [25] Pesaran, Ahmad A, Meckler, Milton, Parent, Yves O., Novosel, Davor. "evaluation of a liquid desiccant-enhanced heat pipe air conditioner", *ASHRAE Transactions*, ASHRAE Atlanta, 1:713-724, 1995
- [26] D.G. Waugaman, A. Kini, and C.F. Kettleborough, "A review of desiccant cooling systems", *Trans. of ASME Journal of Energy Resources Technology*, 115, 1-8, 1993.
- [27] Ullah, M.R., Kettleborough and Gandhidasan, P. "Effectiveness of moisture removal for an adiabatic counterflow packed tower absorber operating with CaCl_2 – air contact system", *Journal of Solar Energy Engineering*, 110(5):98-100, 1988
- [28] A. A. Al- Farayedhi, P. Gandhidasan and M. A. Antar "Performance study of heat and mass transfer in a structured packing liquid desiccant regenerator", *progress in transport phenomena*, The 13th International Symposium on Transport Phenomena, pp:453-457.
- [29] Sanjeev Jain, P.L. Dhar and S.C. Kaushik. "evaluation of liquid desiccant based evaporative cooling cycles for typical hot and humid climates, *Heat Recovery Systems and CHP*, 14(10): 621-632, 1994.
- [30] H.A.Gari, S.E.Aly and K.A Fathalah. "analysis of an integrated absorption/liquid desiccant air conditioning system", *Heat Recovery Systems and CHP*, 10(2): 87-98, 1990.

- [31] Edward N.S, Reinhard Radermacher. "performance analysis of a combined desiccant/absorption air-conditioning system", HVAC & Research, 5(1): 77-84, 1999.
- [32] Ryan, W. Marsala, J. and Griffiths, W., 1989, "laboratory and field experimental results for a residential liquid desiccant dehumidifier," Solar Engineering- Proceedings of the 11 th Annual ASME Solar Energy Conference, San Diego, CA., 353-361, 1989.
- [33] C.F. Kettleborough and D.G. Waugaman, "An alternative desiccant cooling cycle", Journal of Solar Energy Engineering. 117:251-255, 1995.
- [34] Albers, W.F., Beckman, J. R. Farmer, R.W., Gee, K.G., "ambient pressure, liquid desiccant air conditioner", ASHRAE Transactions, 97(2): 603-608, 1991.
- [35] Yadav, Y. K," vapor compression and liquid desiccant hybrid solar conditioning system for energy conservation," Renewable Energy, 6(7): 719-723, 1995.
- [36] Yadav, Y. K and Kuashik, S.C., 1991, " psychometric techno economic assessment and parametric studies of vapor compression and solid liquid desiccant hybrid solar space conditioning systems", Heat Recovery Systems, CHP, 11(6): 563-572.
- [37] L. E. Neilson, Predicting the properties of mixtures, mixing rules in Science and Engineering. Marcel Dekker Inc., New York, 1978.
- [38] Dow Chemical Company, Calcium Chloride Handbook, Michigan, USA, 2001
- [39] T. Uemura. "Studies on the lithium chloride-water absorption refrigeration machines", Technol Report, Kansai University, 9: 71-88, 1967.

- [40] "Hybrid liquid desiccant based vapor compression cooling system", Final Report, KACST Project No. AT-17-30, July 2002.
- [41] G. J. Thuesen and W. J. Fabrycky, Engineering Economy, 8th Ed., Prentice-Hall, 1993.